USE OF HELICAL WIRE CORE TRUSS MEMBERS IN SPACE STRUCTURES

A THESIS SUBMITTED TO
THE GRADUATE SCHOOL OF NATURAL AND APPLIED SCIENCES
OF
MIDDLE EAST TECHNICAL UNIVERSITY

BY

MURAT IŞILDAK

IN PARTIAL FULFILLMENT OF THE REQUIREMENTS
FOR
THE DEGREE OF MASTER OF SCIENCE
IN
CIVIL ENGINEERING

MAY 2009

Approval of the thesis:

"USE OF HELICAL WIRE CORE TRUSS MEMBERS IN SPACE STRUCTURES"

submitted by **MURAT IŞILDAK** in partial fulfillment of the requirements for the degree of **Master of Science in Civil Engineering Department, Middle East Technical University** by,

Prof. Dr. Canan Özgen _____
Dean, Graduate School of **Natural and Applied Sciences**

Prof. Dr. Güney Özcebe _____
Head of Department, **Civil Engineering**

Assoc. Prof. Dr. Uğur Polat _____
Supervisor, **Civil Engineering Dept., METU**

Examining Committee Members:

Prof. Dr. Mehmet Utku _____
Civil Engineering Dept., METU

Assoc. Prof. Dr. Uğur Polat _____
Civil Engineering Dept., METU

Prof. Dr. Süha Oral _____
Mechanical Engineering Dept., METU

Assoc. Prof. Dr. Uğurhan Akyüz _____
Civil Engineering Dept., METU

Assist. Prof. Dr. Özgür Kurç _____
Civil Engineering Dept., METU

Date: May 11, 2009

I hereby declare that all information in this document has been obtained and presented in accordance with academic rules and ethical conduct. I also declare that, as required by these rules and conduct, I have fully cited and referenced all material and results that are not original to this work.

Name, Last name: Murat IŞILDAK

Signature:

ABSTRACT

USE OF HELICAL WIRE CORE TRUSS MEMBERS IN SPACE STRUCTURES

Işıldak, Murat
M.S., Department of Civil Engineering
Supervisor: Assoc. Prof. Dr. Uğur Polat

May 2009, 74 pages

In an effort to achieve lighter and more economical space structures, a new patented steel composite member has been suggested and used in the construction of some steel roof structures. This special element has a sandwich construction composed of some strips of steel plates placed longitudinally along a helical wire core. The function of the helical core is to transfer the shear between the flange plates and increase the sectional inertia of the resulting composite member by keeping the flange plates at a desired distance from each other. Because of the lack of research, design engineers usually treat such elements as a solid member as if it has a full shear transfer between the flanges. However, a detailed analysis shows that this is not a valid assumption and leads to very unsafe results. In this context, the purpose of this study is to investigate the behavior of such members under axial compression and determine their effective sectional flexural rigidity by taking into account the shear deformations. This study applies an analytical investigation to a specific form of such elements with four flange plates placed symmetrically around a helical wire

core. Five independent parameters of such a member are selected for this purpose. These are the spiral core and core wire diameters, the pitch of the spiral core, and the flange plate dimensions. Elements with varying combinations of the selected parameters are first analyzed in detail by finite element method, and some design charts are generated for the determination of the effective sectional properties to be used in the structural analysis and the buckling loads. For this purpose, an alternative closed-form approximate analytical solution is also suggested.

Keywords: Sandwich Beam, Helical Wire Core, Composite Truss Member, Finite Elements, Effective Sectional Inertia

ÖZ

SPİRAL KAFES GÖVDELİ ÇUBUK ELEMANLARIN UZAY YAPISAL SİSTEMLERDE KULLANIMI

Işıldak, Murat

Yüksek Lisans, İnşaat Mühendisliği Bölümü

Tez Yöneticisi: Doç. Dr. Uğur Polat

Mayıs 2009, 74 sayfa

Son yıllarda daha hafif ve ekonomik çelik uzay yapılar elde etmek üzere tasarımda patentli ve sandviç bir yapıya sahip çelik çubuk elemanların kullanılması önerilmektedir. Özellikle çelik çatı tasarımında kullanılan bu özel elemanlar temel olarak spiral bir yay formundaki tel kafes gövde boyunca yerleştirilmiş çelik plaka şeritlerden oluşmaktadır. Bu kompozit yapıda spiral kafes gövde, bir yandan flanş plakaları arasındaki kesme transferini sağlarken aynı zamanda bu plakalar arasındaki mesafeyi belirli bir düzeyde tutarak kesitin atalet momentini artırmaktadır. Bu tip sandviç yapıya sahip elemanların davranışı yakından incelenmemiş olduğundan tasarımı yapan mühendisler genellikle elemanın kesme rijitliği açısından yeterince güçlü olduğu ve dolayısı ile kesme deformasyonunun küçük ve plakalar arasındaki kesme transferinin mükemmel olduğu varsayımından hareket etmektedirler. Ancak bu yaklaşımın geçersiz ve son derecede hatalı olduğu görülmekte ve eleman rijitliğinin analizlere olduğunun çok üzerinde yansıtılmasına yol açarak yapısal güvenlik açısından olumsuz sonuçlar verdiği görülmektedir. Çalışmada bu tür elemanlardan spiral kafes gövde çevresine simetrik olarak yerleştirilmiş dört adet

çelik şerit plakadan oluşan ve adeta kutu kesitli bir çubuk formundaki tipi analitik olarak incelenmiştir. Bu amaçla bu tip elemanların yapısal özelliklerini belirleyen beş temel parametre seçilmiştir. Bunlar spiral gövde ve spiral yay çapları, spiral adımı ve flanş plaka boyutları olarak belirlenmiştir. Bu beş parametrenin değişik kombinasyonlarından oluşan çubuklar önce sonlu elemanlar yöntemi kullanılarak ayrıntılı olarak incelenmiş ve yapısal analiz ve tasarımda kullanılmak üzere elemanların etkin kesit ataletleri ile burkulma dayanımlarını belirlemek üzere abaklar oluşturulmuştur. Bu amaçla alternatif bir yaklaşık analitik yöntem de önerilmektedir.

Anahtar Kelimeler: Spiral Sandviç Kiriş, Spiral Kafes Gövde, Kompozit Çubuk Eleman, Sonlu Elemanlar, Etkin Kesit Ataleti

ACKNOWLEDGMENT

I would like to thank all the people who have helped and inspired me during my master study.

I especially thank to my supervisor, Assoc. Prof. Dr. Uğur Polat for his guidance during my study. His perpetual energy and enthusiasm in research had motivated me. In addition, he was always accessible and willing to help me with my study.

My deepest gratitude goes to my family for their unflagging love and support throughout my life. This thesis would be impossible without them.

TABLE OF CONTENTS

LIST OF TABLES

LIST OF FIGURES

LIST OF SYMBOLS / ABBREVIATIONS

I	Sectional moment of inertia
E	Modulus of elasticity
E_r	Reduced modulus of elasticity
b_f	Flange plate width
t_f	Flange plate thickness
ϕ	Helical core diameter
d_w	Helical wire diameter
K	Effective sectional inertia factor
S	Pitch of the core helix
FEA	Finite Element Analysis
FEM	Finite Element Method

CHAPTER 1

INTRODUCTION

1.1 General

A growing interest in space frame structures has been witnessed worldwide over the last half century. The search for new structural forms to accommodate large unobstructed areas has always been the main objective of architects and engineers. With the advent of new building techniques and construction materials, space frames frequently provide the right answer and satisfy the requirements for lightness, economy, and speedy construction. New and imaginative applications of space frames are being demonstrated in the total range of building types, such as sports arenas, exhibition pavilions, assembly halls, transportation terminals, airplane hangars, workshops, and warehouses.

Space frames are highly statically indeterminate and their analysis leads to extremely tedious computations if carried out by conventional methods. The difficulty of the complicated analysis of such systems contributed to their limited use. However, the introduction of electronic computers has radically changed the whole approach to the analysis of space frames. By using computer programs, it is possible to analyze very complex space structures with great accuracy and less time involved.

The structural pattern of large span steel space structures is built up from basic modules that are repeated throughout the structure The economical importance of the system is that the construction is so simple that simple prefabricated units are mass-produced, easily transported, and erected when required.

1.2 The Use of Composite Sections and Sandwich Beams

Historically, there have been plenty of studies to get rid of the less effective sectional parts such as the web of I shaped sections. The composite section approach is a result of this idea. In the section, the less effective sectional parts are made of weaker and consequently cheaper material. This reduces the cost and the weight of the section.

Sandwich beams, constructed with two stiff, strong face sheets and a lightweight, relatively flexible core, are widely used in various industrial applications demanding a high bending stiffness and strength per unit weight. The relatively large separation introduced by the core and the relatively high axial stiffness of the face sheets aid in effectively increasing the thickness of the sandwich beam, leading to a large bending stiffness per unit weight. Under axial compression, a sandwich beam has a very different failure mechanism than a corresponding monolithic structure. Failure of a sandwich beam under end compression is by a number of competing mechanisms, two of which are the global and local buckling instabilities.

In Euler-Bernoulli beam theory, it is assumed that plane cross sections normal to the axis of the beam remain plane and normal to the axis after deformation. This assumption implies that all transverse shear deformations are zero. However, the effect of transverse shear deformation on bending cannot be neglected when dealing with sandwich beams, having a relatively flexible core due to that the transverse shear deformations become relatively significant.

1.3 Helical Wire Core Truss Member

The idea in the construction of a helical wire core truss members is very similar to the motivation in the design of sandwich beams. In principle, the helical wire core truss member works as an I-shaped beam. However, instead of the web, the shear between the flanges is transferred by a helical wire core (Figure 1 and Figure 2). The main objective is to obtain an alternative element to be used in space frame structures demanding a high axial and bending stiffness and strength per unit weight.

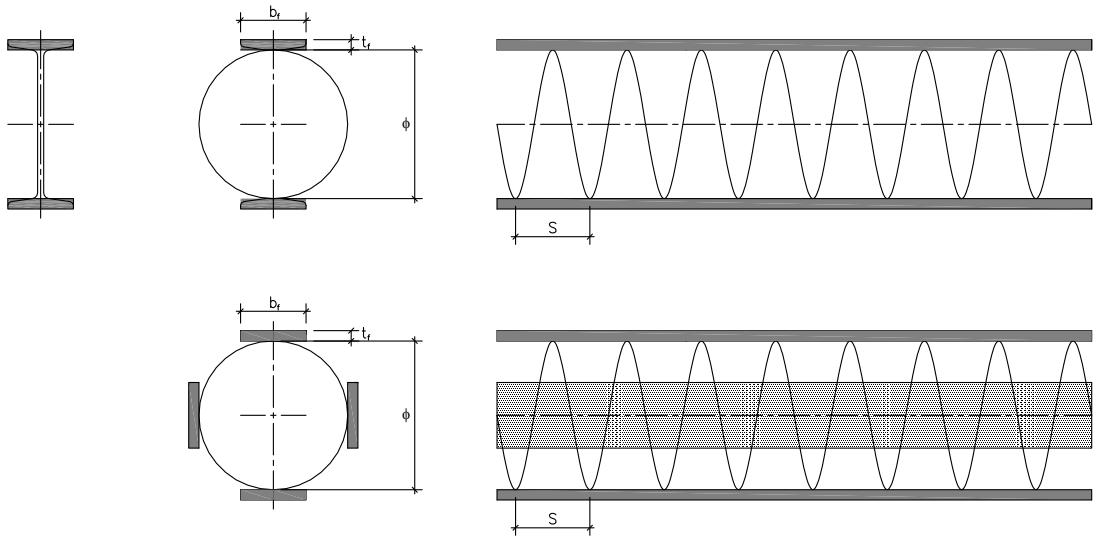

Figure 1 The comparison of helical wire truss member and I beam

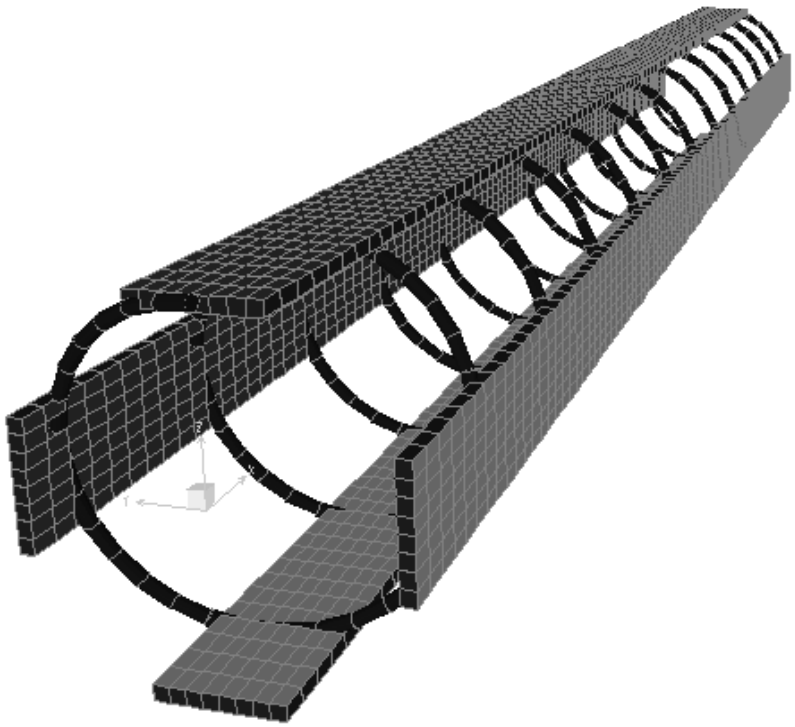

Figure 2 3D view of helical wire truss member

Space frames as a structural form are normally used for large span structures subject to transverse loading. In order to achieve both the optimum use of the material and economy in the design and the efficiency of the resulting load bearing system, they are usually constructed by proper arrangement of axial load members in the form of space trusses. It is also customary to use members with solid sections and more specifically tubular sections as truss elements. Helical wire core truss members may be used in such space frame structures as an alternative to solid and tubular members. For those elements which are subjected to tensile forces, the capacity is controlled by the total yield capacity of the flanges. The shape and size of the helical wire core has very limited and almost negligible contribution on the axial load capacity. However, when they are subjected to compressive forces, the transverse shear deformation of the helical wire core has a significant influence on the element capacity as it controls the element lateral stability.

Another advantage of these members is that they can be formed very easily. This is especially helpful when they are used in curved forms as in the case of roof structures having the shape of a barrel vault (see Figure 3). However, the behavior of curved helical wire core truss members is out of the scope of this study.

Figure 3 Helical wire core truss member used in roof construction.

1.4 Object and Scope of the Study

The object of this study is to investigate in detail the behavior of helical wire core truss members under compressive load. The members are composed of four longitudinal steel flange plates placed around a helical wire core. This sandwich construction of the element has a pronounced effect on its buckling behavior since the wire core is relatively flexible compared to its flange plates and it does not maintain a full shear transfer between the flanges. The level of shear transfer is a function of the relative flexibility of the helical wire core. The shear lag introduced by its deformation under transverse shear leads to a reduction in the flexural stiffness of the member. Therefore, the effective sectional inertia of the member is closely related to the helical wire core structure as well as the flange plate dimensions.

There are basically five parameters defining a specific structure of a helical wire core truss member. These are the core diameter (ϕ), the wire diameter (d_w), the pitch (S) of the wire core, and the width (b_f) and the thickness (t_f) of the flange plates. In order to discover the behavior of helical wire core truss members of every possible size and structure, some practical ranges are prescribed for these parameters and members with different combinations of these parameters are analyzed in detail by the finite element method. The buckling loads are initially calculated for 1000 mm long specimens. The reason is that for members having its basic parameters in the selected practical range, the compressive load capacity of shorter members is normally controlled by the yield capacity of the flanges. The results are presented in a graphical form. These graphs can be used for design purposes. The sectional transverse shear rigidity of a given member can be obtained from these graphs, and using this transverse shear rigidity, the buckling load of longer members with the same structure can easily be calculated. An approximate procedure is also suggested for the calculation of the sectional transverse shear rigidity of a given member without using these graphs and the results are compared with those obtained from detailed finite element analyses.

The scope of the study is limited to the behavior of straight helical wire core truss members under compressive loads only. The behavior of curved members and members which are subjected to transverse loading are out of the scope of this study.

CHAPTER 2

LITERATURE REVIEW

Historically the idea of using two plates separated by a distance is first discussed by Duleau, in 1820 [1], and later by Fairbairn [2]. But it was not used till 1930. In the World War II, sandwich laminates were constructed for the first time with a balsa core for The Mosquito aircraft. This was because of the shortage of other materials and the need of increasing the structural efficiency of the material. Towards the end of World War II, in the late 1940's, some of the theoretical works on sandwich panels were published [3].

The development of core materials has continued from 1940's through today to reduce the weight. The first material used was Balsa which is still in use where weight is not so critical. From 1940's to 1950's the honeycomb core material were developed for the aerospace industry. Honeycomb cores currently offer the greatest shear strength and stiffness to weight ratios, but require care to get the adequate bonding to the faces. However, its high cost has restricted the application of this material in aerospace industry.

The theoretical research has generally preceded the practical application of sandwich constructions from 1940's right through to modern times. The classical solutions for sandwich beams and plates were made by Plantema [4]. As the core of some sandwich beams is typically made of a relatively flexible material, the deformation of the beam causes significant shear strains between panels. Thus, unlike the commonly used homogenous beams with common geometries, shear deformation of the core material must be taken into account in the analysis for sandwich beams to achieve

realistic results. Several beam solutions including shear deformation effects are reported in the literature.

Ettouney and Schmidt [5] solved the plane stress elasticity equations and developed a finite element solution for deep beams, including shear deformation effects. They solved two types of deep beams; one with rectangular cross-section and one with arbitrary cross-section and derived the element stiffness matrix by applying the virtual displacements to the system. They compared the solution with the conventional engineering theory of beam solutions for simple structures and found that the conventional solution underestimates the calculated displacement by up to 23% in cases with beam aspect ratios less than 2.25.

By using well known Timoshenko beam formulation, simpler shear deformation formulations were used. Mucichescu [6] used a displacement formulation and developed a Timoshenko beam element, including shear deformation effects. His solution starts with five degrees of freedom per element. As a fifth degree of freedom, he included the shear deformation with an assumption of any cross section, which is initially plane, and remains plane after the beam deformation [7]. By using static condensation, he obtained a four degree of freedom beam element. Starting with six degrees of freedom, and performing static condensation, Mucichescu [6] reported that the stiffness matrix obtained is identical to that based on a five degree of freedom solution.

The main idea of these transformations was to predict the behavior of the structure faster and easier. There is a continuing research on the development of elements that combine the accuracy of higher order elements with the simple nodal configuration of lower order elements. An effective method in this context has been introduced by Tessler and Dong [8] for Timoshenko beams [9] using lower order shear angles in a base element, they derived a group of constrained elements with fever nodes. In this methodology, displacements and rotations were expressed by polynomials and were later called "anisoparametric interpolation" by Tessler and Hughes [10]. The anisoparametric approach is physically applicable to bending type elements. However, the decrease in the node number of a model makes it necessary to have a

deflection-matching analysis and improve the stiffness of the element. Tessler and Hughes [11] found a new shear correction factor that incorporates both the classical shear correction, and the element properties are determined.

Oral [12] developed a Timoshenko beam using a hybrid stress finite element formulation, which gives accurate displacements and bending moments throughout the beam without any finite element shear correction. The element model provided a powerful tool in the finite element formulations for bending problems.

Using Hamilton's principle, a two node Timoshenko beam was derived by Friedman and Kosmatka [13]. Hamilton principle is a generalization of the principle of virtual displacements into dynamic systems-. Although their formulation is based on the exact shape functions for a static solution, it was successfully adopted in solving dynamic problems. The obtained stiffness matrix is very similar with the one derived by Mucichescu [6]; however there is a single exception; shear shape factor was not considered in Mucichescu's [6] formulation. This was not a problem for short thick beams, but for long slender beams the result was overly stiff. This increase in stiffness is also known as shear locking.

Later on, Kosmatka [14] added the effect of axial force into the formulation through the introduction of a geometric stiffness matrix. With numerical results presented he has shown that the buckling load and the natural frequencies of axially loaded isotropic and composite beams are accurately predicted despite the approximations in the formulation.

Aydogan [15] developed a stiffness matrix for a beam element with shear effect on an elastic foundation using the differential-equation approach for plane-frame analysis. He included the shear effect by a second-order term of the derivative of beam element. This was an exact finite element formulation for a Timoshenko beam on an elastic foundation.

Wang [16] introduced six set of relationships to solve the deflections and stress resultants of single span Timoshenko beams with general loading and boundary

conditions, in terms of corresponding Euler–Bernoulli beam solutions. He established the relationships between deflection gradient, stress resultants and deflection of Timoshenko and Euler-Bernoulli beams for simply supported, clamped free, free clamped, clamped simply supported, simply supported clamped and clamped beams. With the exact relations presented, design engineers do not have to perform more complicated flexural-shear-deformation analysis other than familiar Euler Bernoulli solutions.

Ortuzar and Samartin [17] introduced a consistent finite element formulation for four classical 1-d beam models and found an exact Timoshenko beam finite element solution including axial force effects. They presented a comparative study between the Euler– Bernoulli beam and Timoshenko beam formulations with and without axial force effects.

Bazoune and Khulief [18] noticed that there has been no attempt to find the shape functions of a three dimensional Timoshenko beam element, therefore they introduced the exact shape functions for a three dimensional Timoshenko beam element with no warping effect.

Frostig et al. [19] accounted for core height changes and shear deformation of the core material for sandwich beams in their theory. They used beam theory formulation for the skins and a two-dimensional elasticity theory formulation for the core. They considered the core material as vertically flexible and derived an analytical approach for the deformations and internal forces. They also considered the effect of point of application of external force and concluded that it is important where the load is applied. Recent developments in sandwich beam theories include their work.

Frostig and Baruch [20] presented a buckling analysis of sandwich beams with soft cores, with flexibility effects of the core on overall behavior. They derived behavior equations and appropriate boundary and continuity conditions using perturbation techniques. At a load level of 5% and 10% of the corresponding bifurcation load, the stability of the system is exceeded because of the disbanding skin from the core or peeling effects.

Sokolinsky and Frostig [21] have also included the study of buckling behavior of sandwich panels. They stated that the core properties affect the buckling loads and the corresponding modes of the panel in such a way that the structures with identical boundary conditions but with different cores may undergo different types of buckling such as overall and local as well as interactive loss of stability.

Lee et al. [22] developed a layerwise higher-order for the analysis of the model for thick-cored sandwich beams. The model is based on an assumed cubic variation of the longitudinal displacements in each layer, and a parabolic variation of the transverse shear stress across the composite beam with zero values at the free surfaces.

Other developments include the work of Reddy [23] who developed a layerwise laminated plate bending theory based on Lagrange interpolation functions of the thickness coordinate.

A more general cylindrical plate bending theory was developed by Perel and Palazotto [24]. The theory is equally applicable both to thin or thick faces and to transversely rigid or flexible cores.

The nature of the above listed studies reveals that there have always been efforts to increase the load bearing capacity of structural components by different arrangement of the given amount of material. Sandwich construction is just an example of such an effort in which a relatively lighter, cheaper and flexible core material is used between two or more stronger plates. The resulting structures have been studied over years. The idea of using helical wire just like a flexible core material is an alternative method for these types of structural solutions.

CHAPTER 3

BEHAVIOR OF HELICAL WIRE CORE TRUSS MEMBERS

The behavior of helical wire core truss member under axial compression is studied numerically by the finite element method (FEM). The elastic bearing capacities of the mathematical models are obtained by buckling analysis. The primary issue that has to be addressed when studying buckling of a sandwich structure (herein helical wire core truss member) is the shear deformation of the helical core. Hence, the elastic buckling force for each model must be a function of the member core diameter (ϕ), the pitch (S), the flange width (b_f), the flange thickness (t_f) and helical wire diameter (d_w). Once the reliability is checked for the solution with FEM, the correlation of the input parameters with the elastic buckling force is studied. There must be a functional relationship of the form $f(\phi,S,b_f,t_f,d_w)=y$ whose output y is the elastic buckling load of the member with the selected input parameters. This function may allow the designer to find an approximate solution for the member design, rather than constructing analyzing a complex finite element model of the member.

3.1 Numerical Modeling

The finite element method is used to solve physical problems in engineering analysis and design. It is a technique to turn a physical problem into a mathematical problem. By means of certain assumptions and idealizations, a set of differential equations governing the mathematical model is created and the stresses, deflections and reaction forces etc in objects can be estimated. The technique involves dividing the object into relatively small elements whose individual behavior is easily calculated

until a sufficient accuracy is reached. The behavior of all of the small elements is then put together to estimate the stresses and deflections of the entire object [25].

In the finite element analysis, the structure is discretized or subdivided into a series of elements that are connected to each other at nodal points. The material and element geometric properties are specified to represent the physical properties of the model. Boundary conditions and applied loads are then defined to represent the operating environment for which the structure is to be subjected. The finite element analysis is a simulation tool that enables engineers to simulate the behavior of a structure.

When real life problems are analyzed, a mathematical model should be established. The mathematical model will have some assumptions to reach the solution easier. Engineering comes into play at this stage. Cost effectiveness of a finite element model is the prime factor in problems. There is a continuing research on the development of new elements that combine the accuracy of higher order formulation with the simple nodal configuration of lower order elements.

In this section, the behavior of a helical wire core truss member under axial compressive load is analyzed with finite element modeling. For the sake of simplicity and to accelerate the model building phase, an input generator was programmed in Visual Basic to create analysis model with the selected input parameters.

3.1.1 Geometrical Properties

The structure of helical wire core truss members investigated in this study consists of four steel flange plates and a helical wire core welded to each plate to transfer the shear stresses between the flange plates. The welding of the wire core is done just inside of the member and along the centerline of the flange plates (Figure 4).

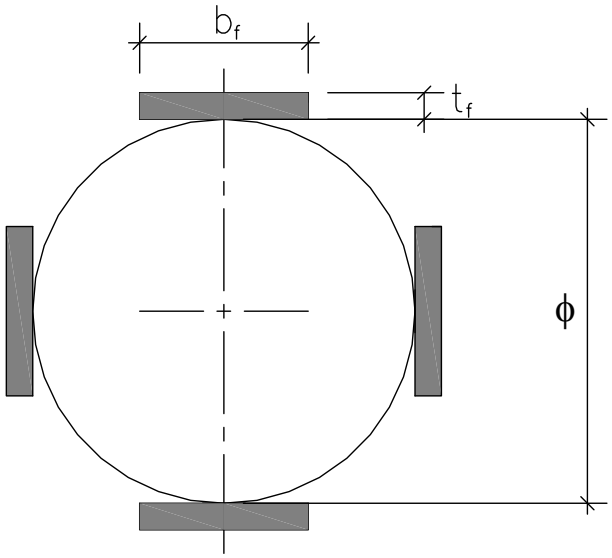

Figure 4 Cross-sectional view of a typical member and the basic parameters

The flange plates of the member are the main substructures that have the most important role in the overall member stiffness. The four plates are located on four quadrants of the core: left, right, top and bottom. Once the member is under an applied moment, one plate tends to have compression and the opposite plate tends to have tension. The distance between the two plates under pressure creates a force couple, hence a moment in the global sense.

In case of bending about one of its principal axes, the side plates increase the flexural stiffness of the member by stiffening the wire core and thus reducing its shear deformations. In addition, they also contribute to bending capacity of the section.

The wire diameter of the helical core has a direct influence on the flexural stiffness of the resulting sandwich member. The level of stresses induced in the helical wire is relatively quite low when the member is subjected to bending. Therefore, as long as the strength demand from the wire core during buckling of such members is concerned, a rather small wire diameter is sufficient for most practical cases. However, its stiffness is vitally important in controlling the effective flexural rigidity

of the member. For this reason, as large wire diameter as economically feasible is beneficial. Considering the ease of manufacturing of the helical core, the range of plain wire diameters to be investigated in this study is selected between 6.0 mm to 10.0 mm.

The pitch (S) of the helical core also has a direct effect on the flexural stiffness of the resulting sandwich member. The amount of shear deformation per unit length of the member is inversely proportional to the pitch of the helical core. Moreover, it is the minimum distance of the welded joints along each flange plate (Figure 5). It is a parameter selected by the design engineer. Apparently, once selected, the pitch is constant along the helical core. The number of welded joints per unit length of the member increases as the pitch gets smaller. This in turn increases the labor involved in the production of the element. Therefore, the designer must think of the ease and the labor cost of manufacturing in selecting this parameter.

The pitch (S) is very critical for the member stability as well. The unsupported length of the flange plates increases with increasing pitch and this may cause local buckling of some of the plates under compression.

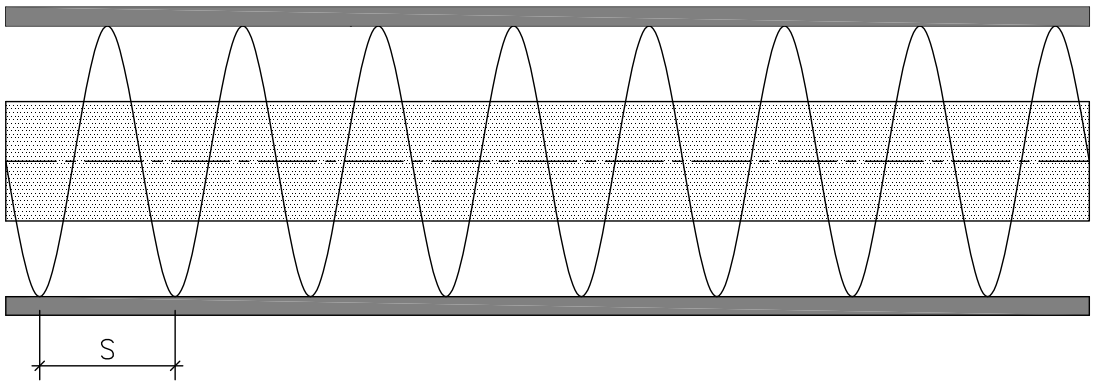

Figure 5 Pitch of the spiral core

The results of a preliminary study show that the shear deformation of the wire core becomes excessively large for the selected range of the wire diameter when the core diameter exceeds 400 mm. Therefore, the core diameter of the members investigated in the study is selected between 20 mm to 400 mm. Finally, the width and the thickness of the flange plates are selected in a range between 20 mm to 50 mm and 4 mm to 8 mm respectively.

3.1.2 Finite Element Modeling

The subject member is structurally composed of four steel plates and a spiral wire core. The plates are subject to axial force and bending. There are two alternative ways of modeling the plates. The flange plates can either be modeled by using two-node three dimensional line elements or by using four-node three dimensional plane elements. The finite element models by these two approaches are studied in detail and the assumptions for each model are as follows.

In case of using four-node plane elements for the flange plates, the mathematical formulation of the elements must be such that; model can capture both the axial and the bending response by the flange plates of the actual structure. Therefore, the plane elements must be capable of representing both the membrane and the plate bending modes of behavior. For this reason, four-node shell elements are preferred to model the flange plates (Figure 6).

The finite element analysis program SAP2000 [27] is used to solve the mathematical finite element model. In SAP2000 [27], there are two possible formulations for the plate bending mode of the element. For thick plates, the transverse shear deformations are significant and the more complex thick-plate (Mindlin/Reissner) formulation require. However, for thinner plates the effect of transverse shear deformations is negligible. Therefore, a thin-plate (Kirchhoff) formulation, in which the transverse shear deformations are neglected, is sufficient [26]. The thickness of the flange plates considered in this study is relatively small and a plate bending element based on thin-plate formulation will be sufficient.

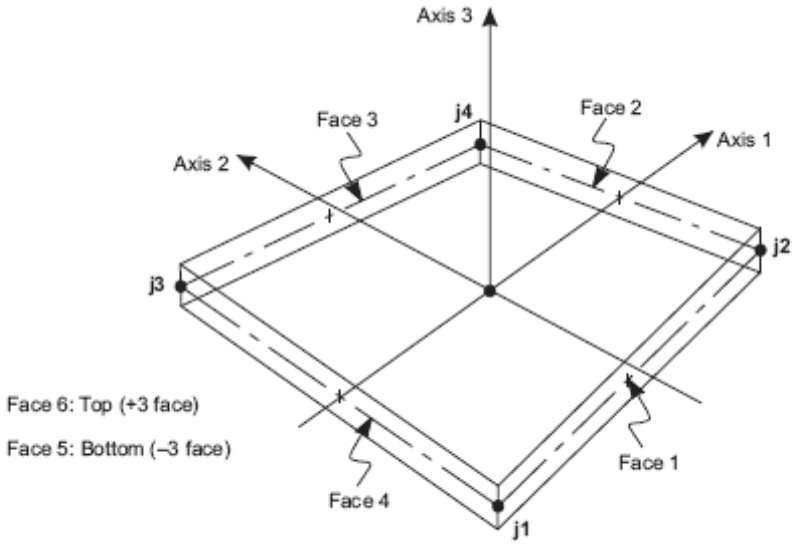

Figure 6 Four- node quadrilateral shell element used for the flange plates [26]

In case of using two node line elements to represent the flange plates of the member, the mathematical model is simpler. It consists of frame elements as flange plates with bending rigidity “EI” and axial rigidity “EA”, where “I” is the moment of inertia of each rectangular flange and “A” is the gross area of the rectangular flanges.

In both mathematical models, two node frame elements with circular cross-section are used to represent the wire core portion of the member. The frame elements of the wire core are connected to flange plates at some discrete points along the centerline of the plates, as shown in Figure 7 and Figure 8.

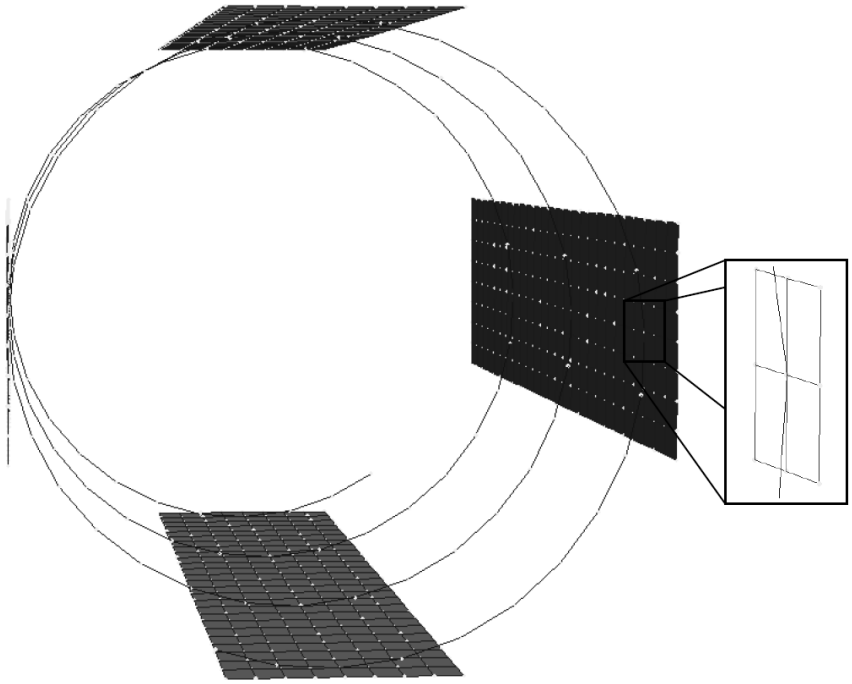

Figure 7 Connection of the frame elements of the wire core and the shell elements of the flange plates

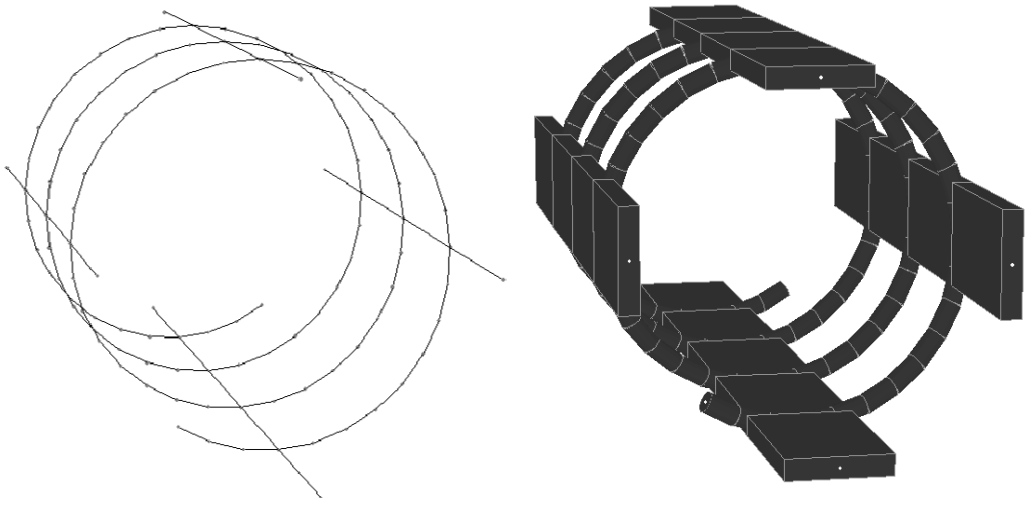

Figure 8 Connection of the frame elements of the wire core and the flange plates

The finite element model building phase of the wire core members is automated by an input generator which is programmed in Visual Basic. The interface of the input generator can be seen in Figure 9.

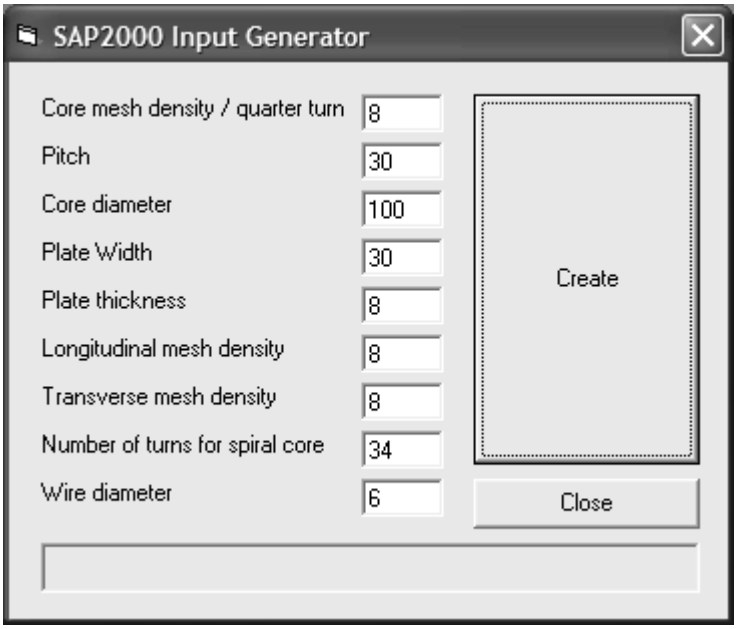

Figure 9 SAP2000 Input generator Graphical User Interface

Core mesh density / quarter turn: The helical wire of the core is divided into a number of small frame elements with 6 degree of freedom at each end. This is the number of divisions per quarter turn of the helical core. For the models used in this study, the parameter is selected as 8. Hence; 8x4=32 frame elements are used for a full turn of the helical wire core.

Pitch: Pitch (S) of the helical wire is an independent parameter for each model.

Core diameter: This is the distance between two opposing flange plates, i.e. the diameter of the helical wire core (ϕ).

Plate width: The width of flange plates (b_f).

Plate thickness: The thickness of flange plates. It is the bending and membrane thickness of each shell element used for the flange plates (t_f).

Longitudinal mesh density: This is a parameter used for the shell models. It is the number of elements along the flange plates between two successive connection points to wire core. It is taken as 8 in the finite element models used in this study.

Transverse mesh density: This is another parameter used for shell models. It is the number of elements used across the flange plates It is taken as 8 in the finite element models used in this study.

Number of turns for spiral core: An integer value by which the length of the member can be adjusted by changing its value. One full turn is equal to the pitch of the helical core. The nearest integer value is used for each member.

Wire diameter: The wire diameter of the helical core. It gives the cross-sectional geometry of the frame elements used in the FE model for the wire core (d_w).

The mathematical model used for the calculation of the buckling load of wire core truss members is shown in Figure 10. The buckling analyses are performed to obtain the eigen-values corresponding to first three buckling modes of each model under compression without eccentricity. As an initial concentric axial load 1000 Newton is applied through thick and relatively rigid end plates. The function of these end plates is to enforce plane deformation state at the ends of the member which is anticipated and assumed to be the case in practical applications. After buckling analysis, the calculated first mode (lowest) eigen-value is multiplied by the initial load to obtain the actual buckling load of the member (P_{crFEM}).

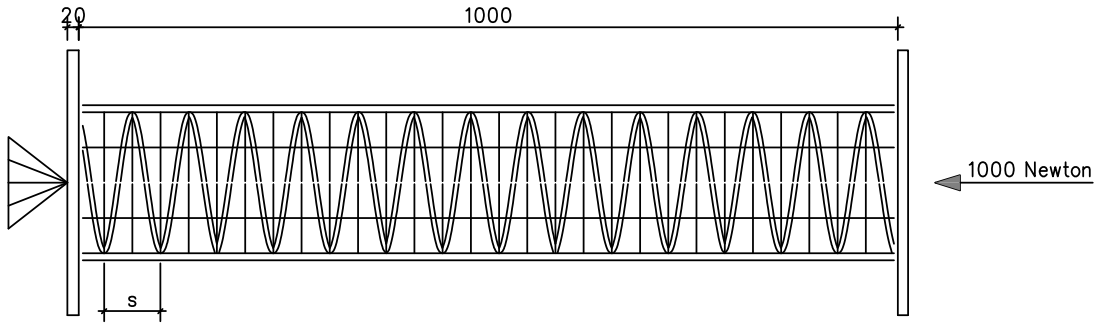

Figure 10 Mathematical model for the buckling analysis.

3.1.3 Basic Failure Modes

There are basically two possible modes of failures of wire core truss members under axial load: the material failure by reaching the yield capacity of the section under either tension or compression and geometric failure by loosing its stability under compressive loads.

The axial load is mainly resisted by the flange plates. The helical wire core obviously has a negligible contribution to the axial yielding capacity of the member. The axial force is equally shared by the four flanges and each flange plate is subjected to an axial stress of $\sigma = \frac{P}{4b_f t_f}$. Unless there is a loss of stability, the ultimate axial load capacity of the member can be calculated by checking if $\sigma \leq \sigma_{yield}$.

The results of the finite element analyses performed on the wire core truss members with its basic parametric values in the practical range selected in this study reveal that the ultimate capacity of such members under axial compressing is normally reached by the loss of its stability. A close examination of the buckling modes of the members indicate that the buckling instability of the members is started mostly in one of three basic modes:

1. Flexural Global Buckling

2. Flexural Local Buckling

3. Torsional Global Buckling

3.1.3.1 Flexural Global Buckling Mode of Failure

Depending on the member length, longer specimens usually loose their stability in the flexural global buckling mode. In other words, as the specimen gets longer, the mode of instability tends to be flexural global buckling. This is the usual mode of buckling for elements having their basic parameters in the practical range selected in this study, if the element length is 1000 mm or longer. The buckling shape is shown in Figure 11.

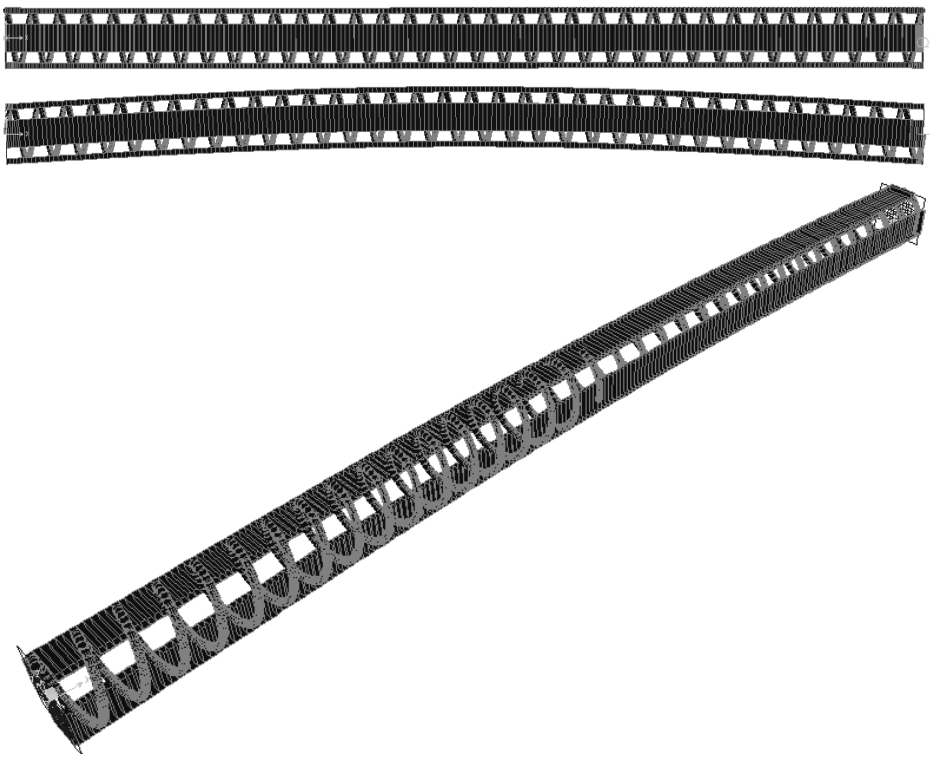

Figure 11 Flexural global buckling mode of failure

3.1.3.2 Flexural Local Buckling Mode of Failure

This becomes the dominant mode of buckling mode when the pitch and the core diameter are large, the wire diameter is small and the flange plates are relatively stiff. In this case, the wire core functions as an elastic foundation with a low modulus of subgrade reaction and the buckling is similar to that of a column supported only transversely by flexible elastic springs. The buckling mode is visually depicted in Figure 12.

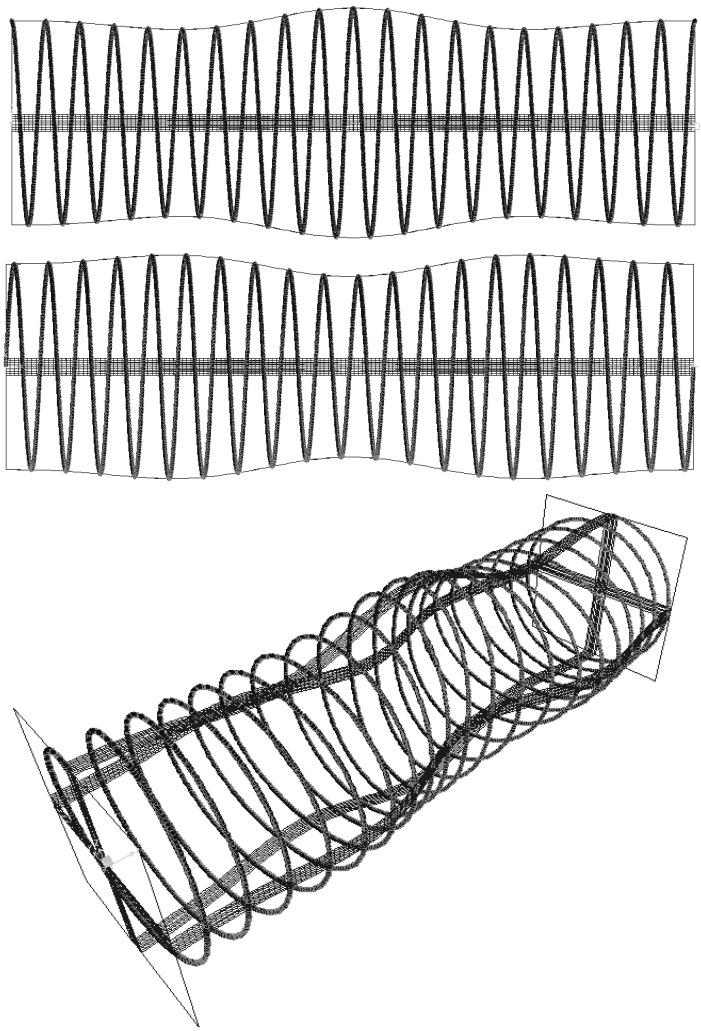

Figure 12 Flexural local buckling mode of failure

3.1.3.3 Torsional Global Buckling Mode of Failure

This mode of instability is observed in the short wire core truss members when the wire diameter and the pitch are large while the core diameter is relatively small. A typical buckling shape is shown in Figure 13.

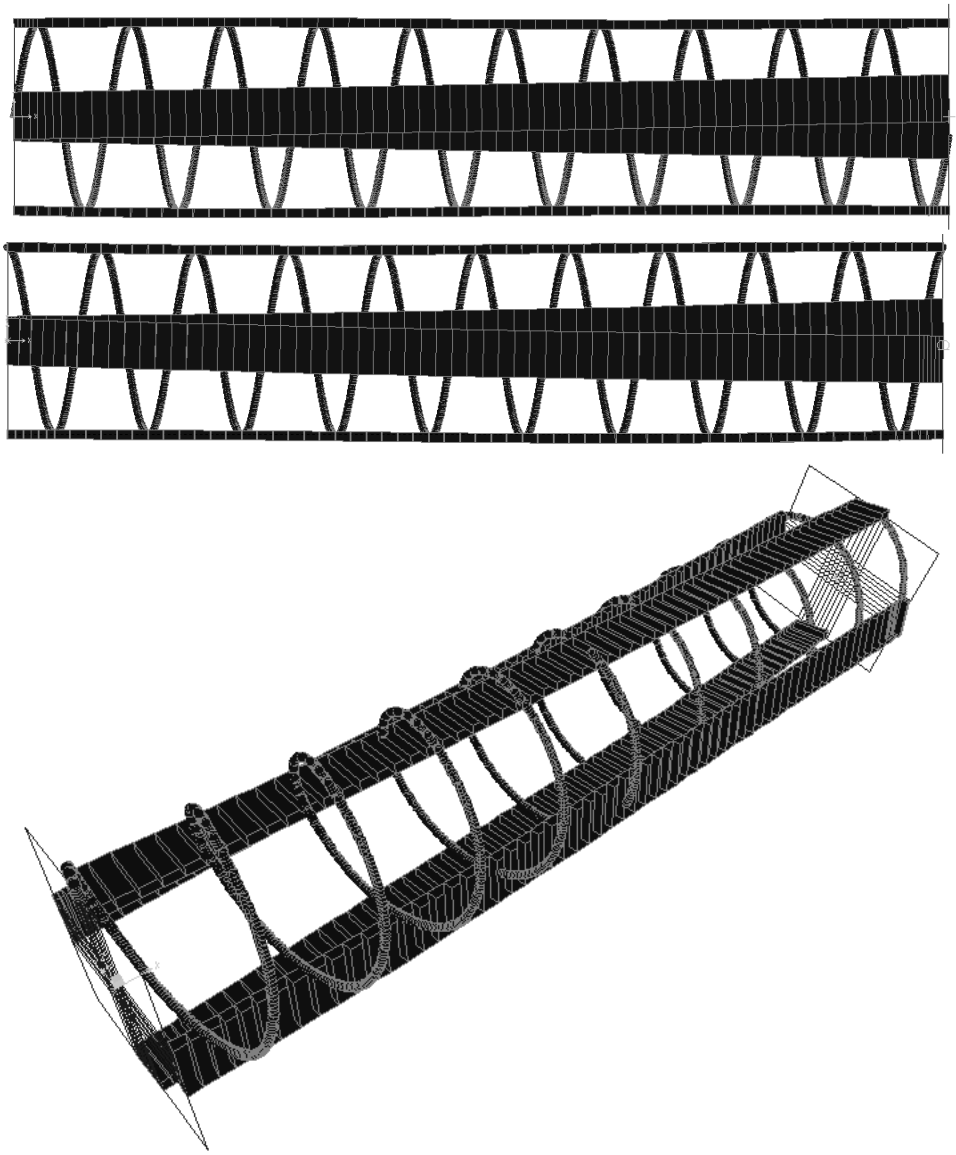

Figure 13 Torsional global buckling mode of failure

3.2 Analytical Approach

The basic knowledge of the mechanics of materials states that the buckling of a structural member depends on several parameters for an ordinary beam. The most important of these parameters are the modulus of elasticity E, the sectional moment of inertia I in the buckling plane, and the effective length of the member. The effective length is a parameter which depends on the actual unsupported length of the member and the boundary conditions.

In order to calculate the buckling load of a member analytically, several assumptions are made. An ideal member under compression must be initially straight with a perfect geometry, and the applied compression force must be perfectly concentric without any eccentricity. If the member is homogenous with a flexural rigidity of EI, the problem may be reduced to an eigen-boundary-value problem.

The buckling load according to the Euler-Bernoulli beam theory is given by

$$P_{cr} = \frac{\pi^2 EI}{L_{eff}^{\ 2}} \tag{3.1}$$

In the case of helical wire core truss member under compression, most of these assumptions are valid and the derivations are similar. However, in the buckling analysis of sandwich columns, herein the helical wire core truss members, the transverse shear deformations must be taken into account. Because of the lack of perfect shear transfer, the buckling load of the member is decreased compared with the ordinary Euler buckling situation. If there were full shear transfer between the plate components, the basic assumption of the Euler-Bernoulli beam theory namely the assumption of plane sections remain plane would be valid and the flexural capacity would be directly proportional to the square of the helical core diameter (ϕ). In this case, the moment of inertia of the section would be dependent on the sectional area of the plates and the distance of the plates to the center of mass of the member. In other words, the moment of inertia of a member calculated by assuming perfect shear transfer is the maximum possible moment of inertia of wire core truss

members. The effective moment of inertia is a function of the resulting transverse shear deformations and can be related to the calculated moment of inertia based on perfect shear transfer as follows:

$$K = \frac{I_{effective}}{I_{calculated}} \leq 1 \tag{3.2}$$

The contribution to the cross-sectional moment of inertia of the wire core member of each flange plate can be calculated as:

$$I = \frac{1}{12} b_f {t_f}^3 + b_f t_f {y_d}^2 \tag{3.3}$$

where b_f and t_f are the width and the thickness of flange plate respectively, and y_d is the distance between the centroids to the wire core element and the flange plate.

Considering the arrangement of the flange plates around the wire core and ignoring the transverse shear deformation of the core, the theoretical moment of inertia of the member can be expressed as:

$$I = 2\left(\frac{1}{12} b_f {t_f}^3 + \frac{1}{12} b_f {t_f}^3\right) + 2\left(b_f t_f \left(\frac{\phi + t_f}{2}\right)^2\right) \tag{3.4}$$

The numerical analyses and theoretical studies show that when the transverse shear deformations are present the effective flexural rigidity $EI_{effective}$ of the helical wire core truss member is obviously smaller than its theoretical value of $EI_{calculated}$. Hence, the bearing capacity of the member is lower. The member buckles under smaller loads than expected by the Euler formula. Just like the sandwich beams and panels, this decrease in buckling load capacity can be formulated to predict the actual behavior of the member under axial compression.

3.3 An Approximate Procedure for the Calculation of the Critical Load Related to the Flexural Global Buckling Mode of Failure

Assuming that the mode of instability will be flexural global buckling, an analytical procedure can be devised for the calculation of the critical buckling load (P_{cr}) of a pin-ended helical wire core truss member, including the influence of transverse shear deformations if some additional simplifying assumptions are made.

As far as the structural behavior of the helical wire core truss member during buckling about one of its principal axes is concerned, the element can be regarded as composed of two independent substructures as shown in Figure 14.

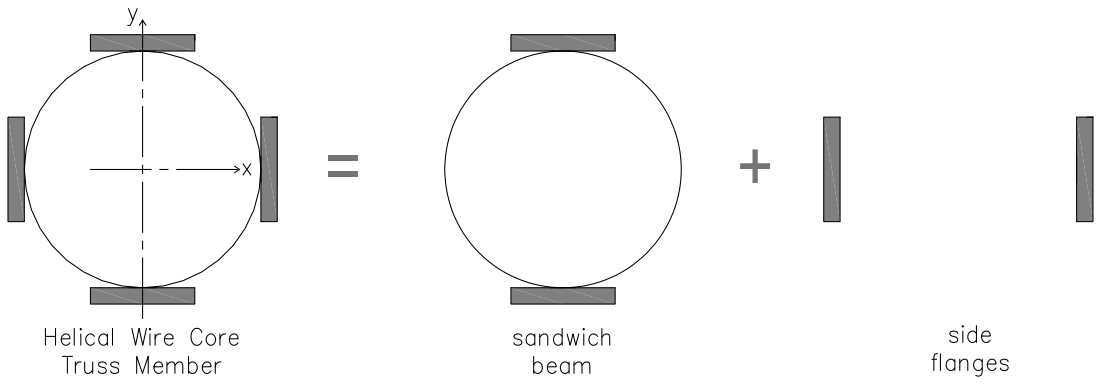

Figure 14 The wire core truss member represented as a combination of two substructures

The substructure labeled as “sandwich beam” in Figure 14 is composed of the wire core and the two of the opposing flanges on either side of the bending axis during buckling. The substructure labeled as “side flanges” is composed of the remaining flanges parallel to buckling plane which are assumed to act independent of the first

substructure. The first substructure will act as a sandwich panel during buckling when the buckling is about a horizontal axis and the shear rigidity of the helical wire core has a key influence on the buckling capacity.

After separation of the member into two independent substructures as described above, the critical buckling load P_{cr} of the helical wire core truss member can be obtained by the superposition of the critical loads of each substructure.

$$P_{cr} = P_{cr(sandwich)} + P_{cr(side)} \tag{3.5}$$

There is nothing special about buckling of the side flanges and the Euler buckling load is valid for this substructure;

$$P_{cr(side)} = \frac{\pi^2 E I_{side}}{(\lambda L)^2} \tag{3.6}$$

where, the modulus of elasticity for steel is E=200000 MPa, the effective length factor for pin-ended member is $\lambda = 1$, and I_{side} is given by

$$I_{side} = 2\left(\frac{1}{12} t_f b_f^{\,3}\right) \tag{3.7}$$

For calculating the critical buckling load of the sandwich beam substructure, $P_{cr(sandwich)}$ the shear effect on the buckling capacity should be known. For a pin-ended column the total lateral deflection y of the centerline is the result of two components as shown in Figure 15

$$y = y_1 + y_2 \tag{3.8}$$

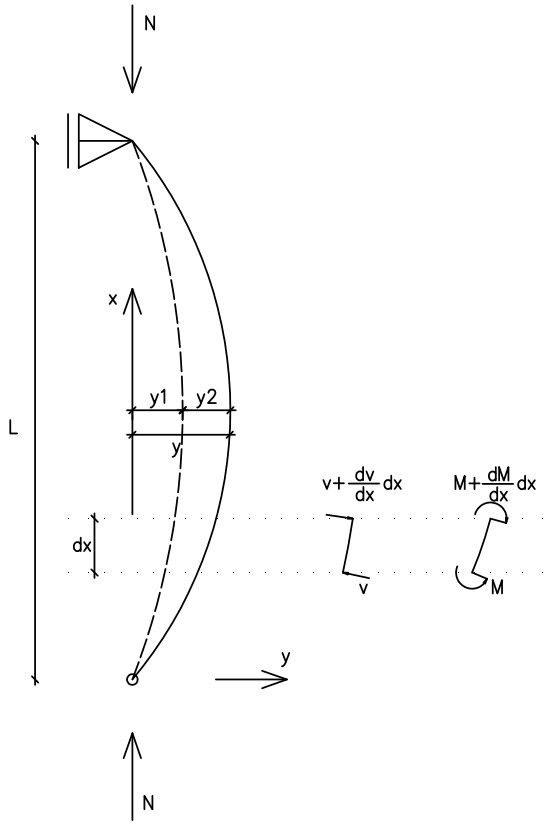

Figure 15 Deflection of pin-ended sandwich column during buckling

The deflection y_1 is the result of the bending moment M, the deflection y_2 is the result of the shearing force V. Using elastic theory the curvature due to the bending moment M is:

$$\frac{d^2y_1}{dx^2} = -\frac{M}{EI} = -\frac{Ny}{EI} \tag{3.9}$$

where E is the modulus of elasticity and I is the moment of inertia of the cross-section.

The slope due to the shearing force V is as follows:

$$\frac{dy_2}{dx} = \frac{V}{GA_s} = \frac{N}{GA_s}\frac{dy}{dx} \tag{3.10}$$

where G is the shear modulus, A_s is the shear area of the cross-section.

The curvature due to the shear force V is:

$$\frac{d^2y_2}{dx^2} = \frac{N}{GA_s}\frac{d^2y}{dx^2} \tag{3.11}$$

The total curvature of the buckling curve due to moment and shear is:

$$\frac{d^2y}{dx^2} = \frac{d^2y_1}{dx^2} + \frac{d^2y_2}{dx^2} = -\frac{Ny}{EI} + \frac{N}{GA_s}\frac{d^2y}{dx^2} \tag{3.12}$$

After rearranging the terms

$$\frac{d^2y}{dx^2} + \frac{N}{\left(1 - \frac{N}{GA_s}\right)EI}y = 0 \tag{3.13}$$

Solving the differential equation:

$$\frac{N}{\left(1 - \frac{N}{GA_s}\right)EI} = \frac{\pi^2}{L^2} \tag{3.14}$$

$$N_{cr(teo)} = \frac{\pi^2 EI_{sandwich}}{L^2} \tag{3.15}$$

where

$$I_{sandwich} = 2\frac{1}{12}b_f t_f{}^3 + 2b_f t_f\left(\frac{\phi}{2}\right)^2 \tag{3.16}$$

$N_{cr(teo)}$ in Equation (3.15) is the Euler buckling load when the shear deformation of the core is neglected. Then, the buckling load of the "sandwich beam" substructure including the transverse shear deformations of the wire core can be expressed as

$$P_{cr(sandwich)} = \frac{1}{\frac{1}{N_{cr(teo)}} + \frac{1}{S_v}} = N_{cr(teo)} \frac{1}{1 + \frac{N_{cr(teo)}}{S_v}} \tag{3.17}$$

where $S_v = GA_s$ is the shear rigidity of the wire core to be calculated.

Therefore, the problem of calculating the buckling load of the "sandwich beam" substructure is reduced to calculation of equivalent shear rigidity S_v for the helical wire core between the flanges.

The value of S_v for the wire core is a function of the pitch (S), the wire diameter (d_w), and the core diameter (ϕ). In order to simplify the calculation of the shear rigidity, S_v, an equivalent structural model of the helical wire core is used in which the one full turn of the helical wire is treated as two battens between the flange plates of the "sandwich beam" substructure. The resulting ladder model for the "sandwich beam" substructure is shown below, Figure 16 and Figure 17.

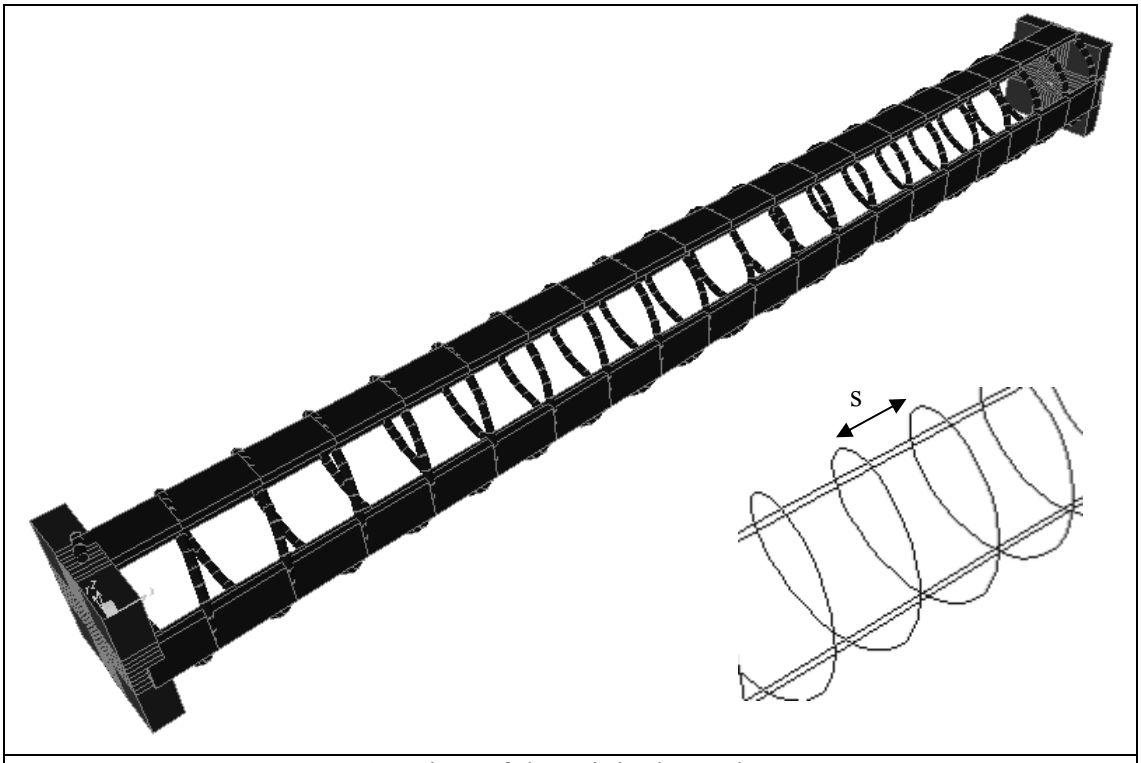

3D view of the original member

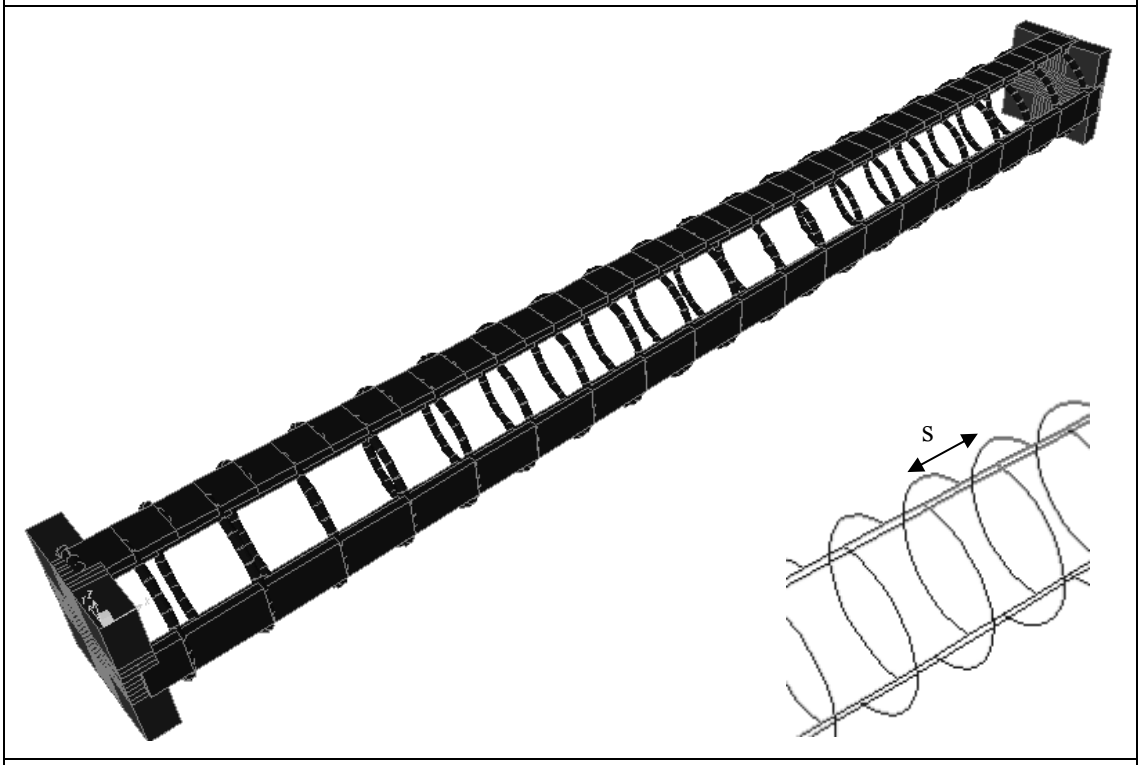

3D view of the equivalent ladder

Figure 16 Simplified ladder representation of the “sandwich beam” substructure

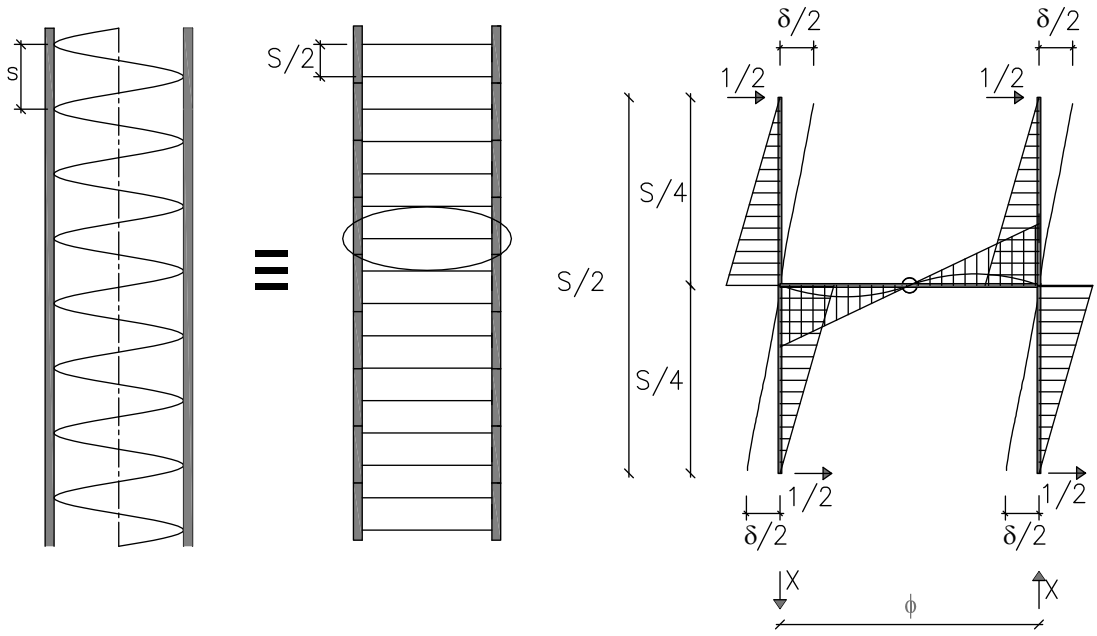

Figure 17 Shear deformation of "sandwich beam" substructure under unit shear

In Figure 17, the free body diagram of one step between two inflection points of the member is shown.

From force equilibrium, the value of x can be calculated as

$$\frac{1}{2}\frac{S}{2} = \frac{\phi}{2}x \Rightarrow x = \frac{S}{2\phi} \tag{3.18}$$

Using the virtual work principle, the displacement δ due to unit transverse shearing force of the wire core can be obtained as

$$\delta = 4\int_0^{S/4} \frac{1}{2}\frac{x}{EI_{flange}}\frac{1}{2}x\,dx + 2\int_0^{\phi/2} \frac{S}{2\phi}\frac{y}{EI_{wire}}\frac{S}{2\phi}y\,dy \tag{3.19}$$

$$\delta = \int_0^{S/4} \frac{x^3}{3EI_{flange}} + \int_0^{\phi/2} \frac{S^2}{6\phi^2} \frac{y^3}{EI_{wire}} \tag{3.20}$$

$$\delta = \frac{S^3}{192EI_{flange}} + \frac{S^2\phi}{48EI_{wire}} \tag{3.21}$$

The shear rigidity is

$$\frac{1}{S_v} = \frac{\delta}{S/2} = \frac{S^2}{96EI_{flange}} + \frac{S\phi}{24EI_{wire}} \tag{3.22}$$

where

$$I_{flange} = \frac{1}{12} b_f t_f^{\,3} \tag{3.23}$$

$$I_{wire} = \frac{\pi d_w^{\,4}}{64} \tag{3.24}$$

The shear rigidity S_v is the major parameter for the transverse shear effect of the helical wire core truss member. P_{cr} can then be calculated easily after the calculation of the shear rigidity S_v given above. A similar approach is proposed in Eurocode 3 [28] for built up columns.

3.4 Prediction of Element Buckling Loads by Finite Element Analysis

The input generator was used to create a set of finite element models in which shell elements are used for the flange plates and another set of models, in which frame elements are used for the flange plates. The comparison of the analysis results show that the models in which the flange plates are represented by frame elements give similar results with the models in which shell elements are used. However, when the flange plates get thicker and wider the predictions of the two models start to deviate from each other.

Regarding the basic parameters of the helical wire core members, some range of prescribed values are deemed appropriate in practical applications and used in the study. These are listed in Table 1. For the values of the parameters in the range prescribed in Table 1, the predicted buckling modes are the same and the difference in the predicted buckling loads is very small. Therefore, it is decided to model the flange plates by frame elements.

Table 1 Parametric values of wire core truss members used in the study

Member Parameters	Helical Core Diameter ϕ (mm)	Pitch S (mm)	Plate width b_f (mm)	Plate thickness t_f (mm)	Wire Diameter d_w (mm)
Parameter Values used in the Study	20 30 40 50 60 70 80 90 100 120 140 160 180 200 250 300 350 400	10 20 30 40 50 60 70 80 90 100 150 200 250	20 25 30 35 50	4 6 8	6 8 10

A total of 10530 finite element models are generated for every combination of the basic parameters listed in Table 1 and solved for buckling loads.

The influence of the parameters on the bearing capacity of the member gives a better understanding of the behavior of the member. In order to display the influence of the

pitch and the core diameter on the buckling capacity, several graphs are generated in Figure 18 through Figure 32 and presented on the following pages. The sensitivity of the element buckling load to related parameters can be seen on these graphs.

In order to better demonstrate the influence of each parameter on the element buckling load the specimens having identical flange dimensions are plotted on the same graphs. For instance, in Figure 18, all specimens have identical flange plate dimensions of 20x4 mm. In each graph, a family of curves is presented, each for a different pitch of the helical wire core. This makes it possible to observe the influence of the core pitch on the element behavior. Moreover, in order to see the relative influence of the core wire diameter on the element behavior, two separate graphs are presented in each figure; one with a helical wire diameter of d_w = 6 mm, the other for a helical wire diameter of d_w = 10 mm.

It is clearly seen that the buckling loads predicted by the proposed approximate scheme and the ones predicted by the finite element solutions are almost identical to each other for a range of parameters indicated on the graphs by a transition line in Grey. It is observed that, for parametric combinations lying below this line, the element buckling loads are somewhat smaller than those predicted by the proposed scheme. A close examination shows that the reason for this discrepancy is due to the fact that the mode of buckling is either local or lateral torsional for those combinations of the member parameters.

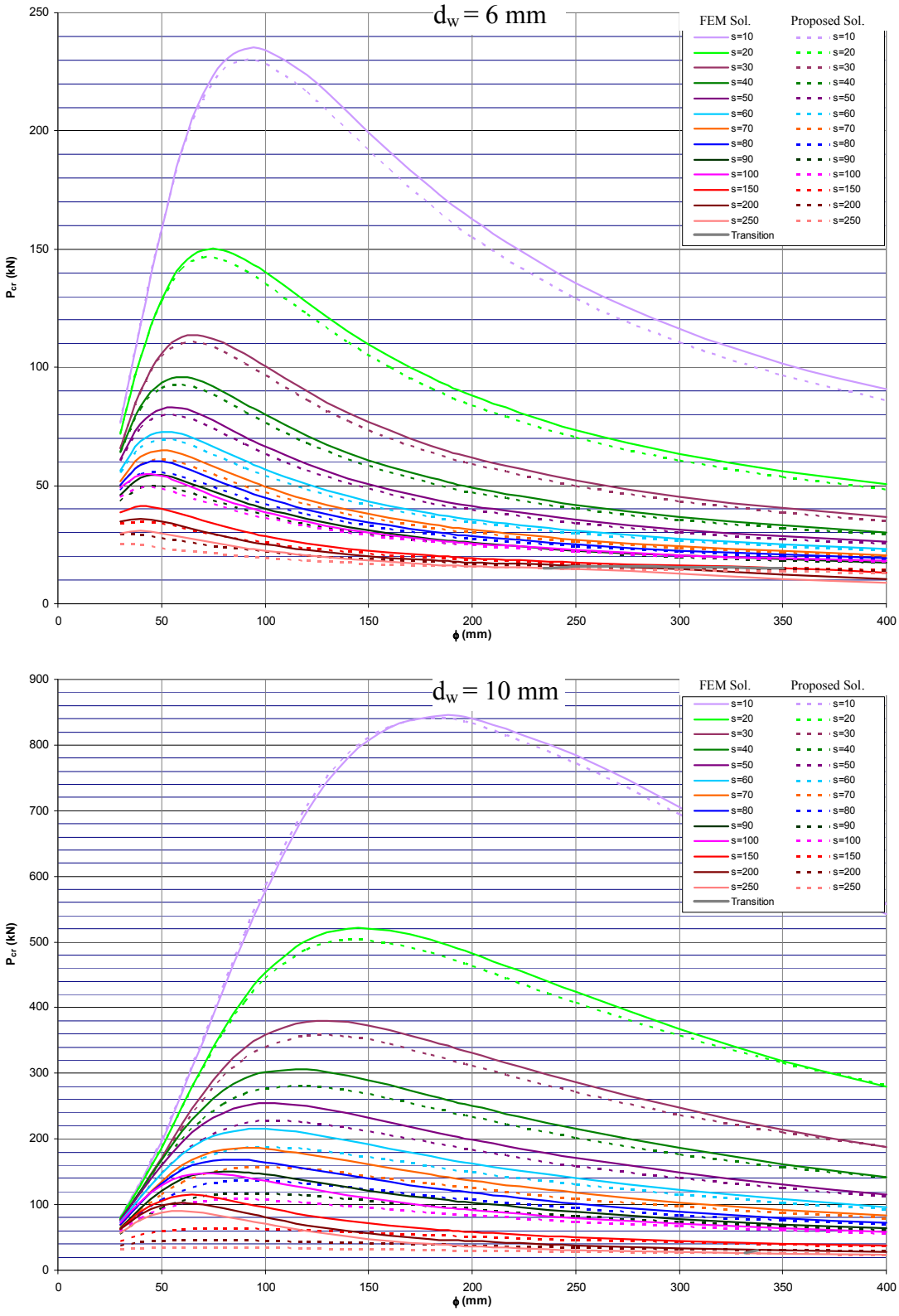

Figure 18 Buckling load of 1000mm members for 20x4mm flange plates

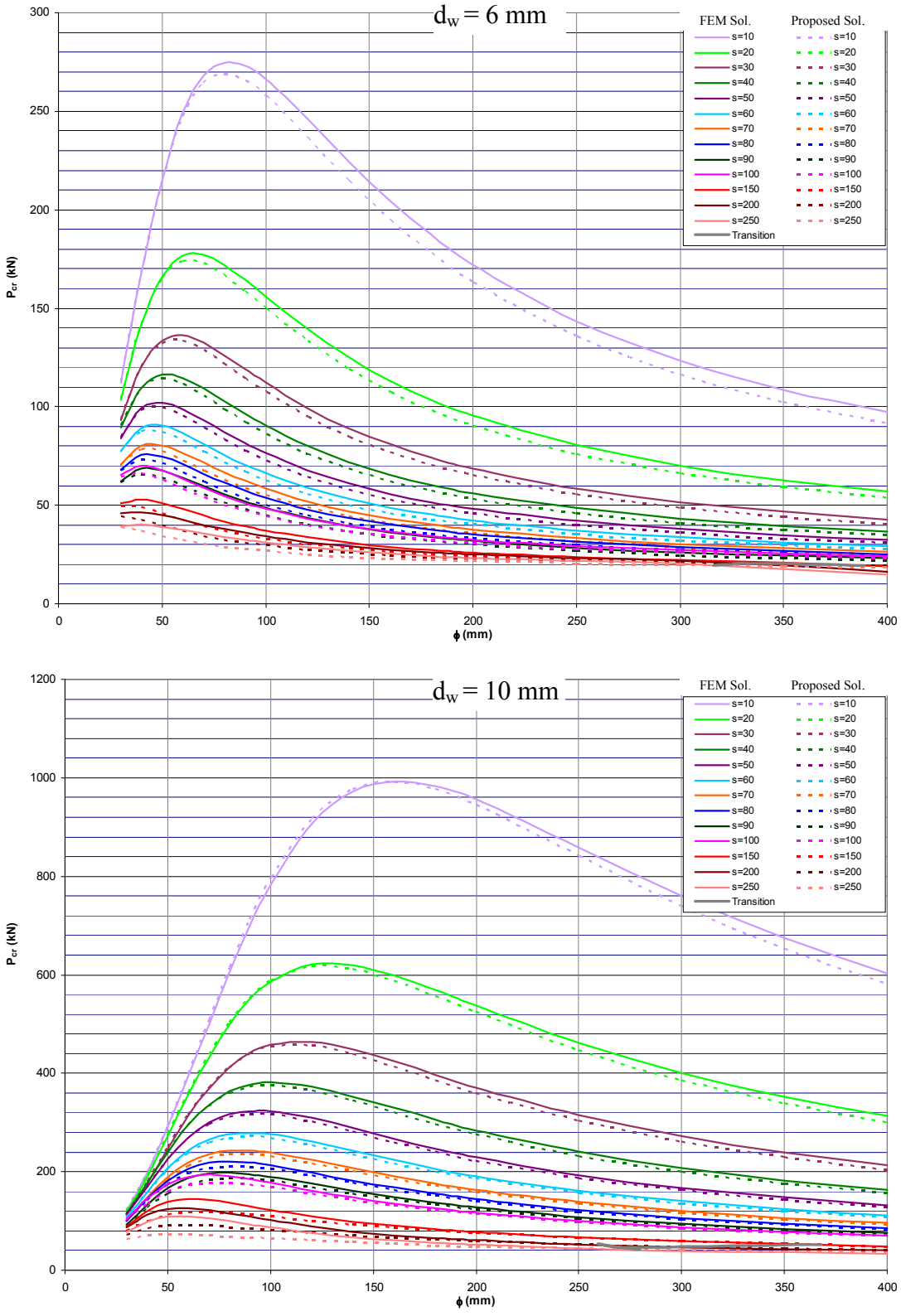

Figure 19 Buckling load of 1000mm members for 20x6mm flange plates

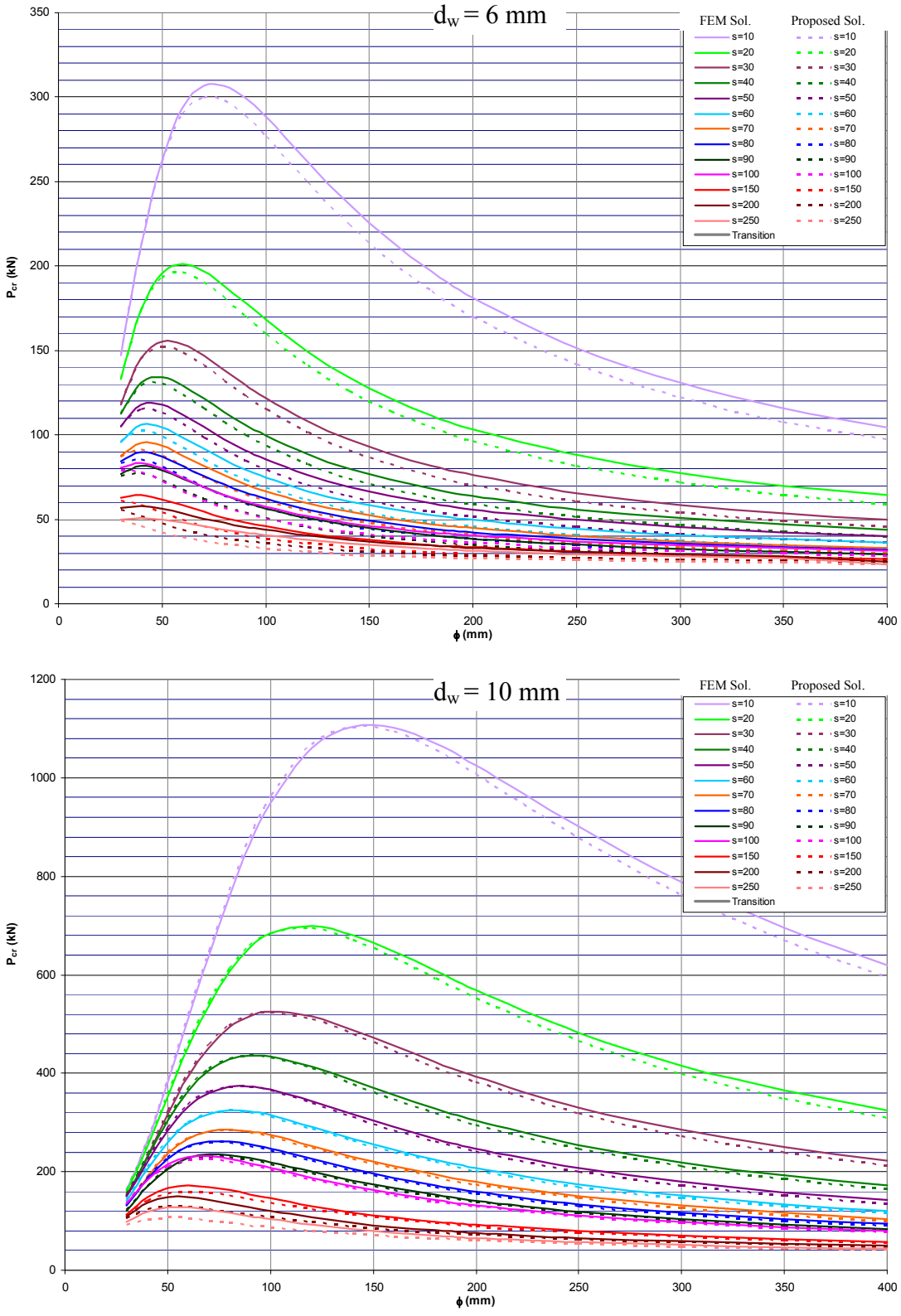

Figure 20 Buckling load of 1000mm members for 20x8mm flange plates

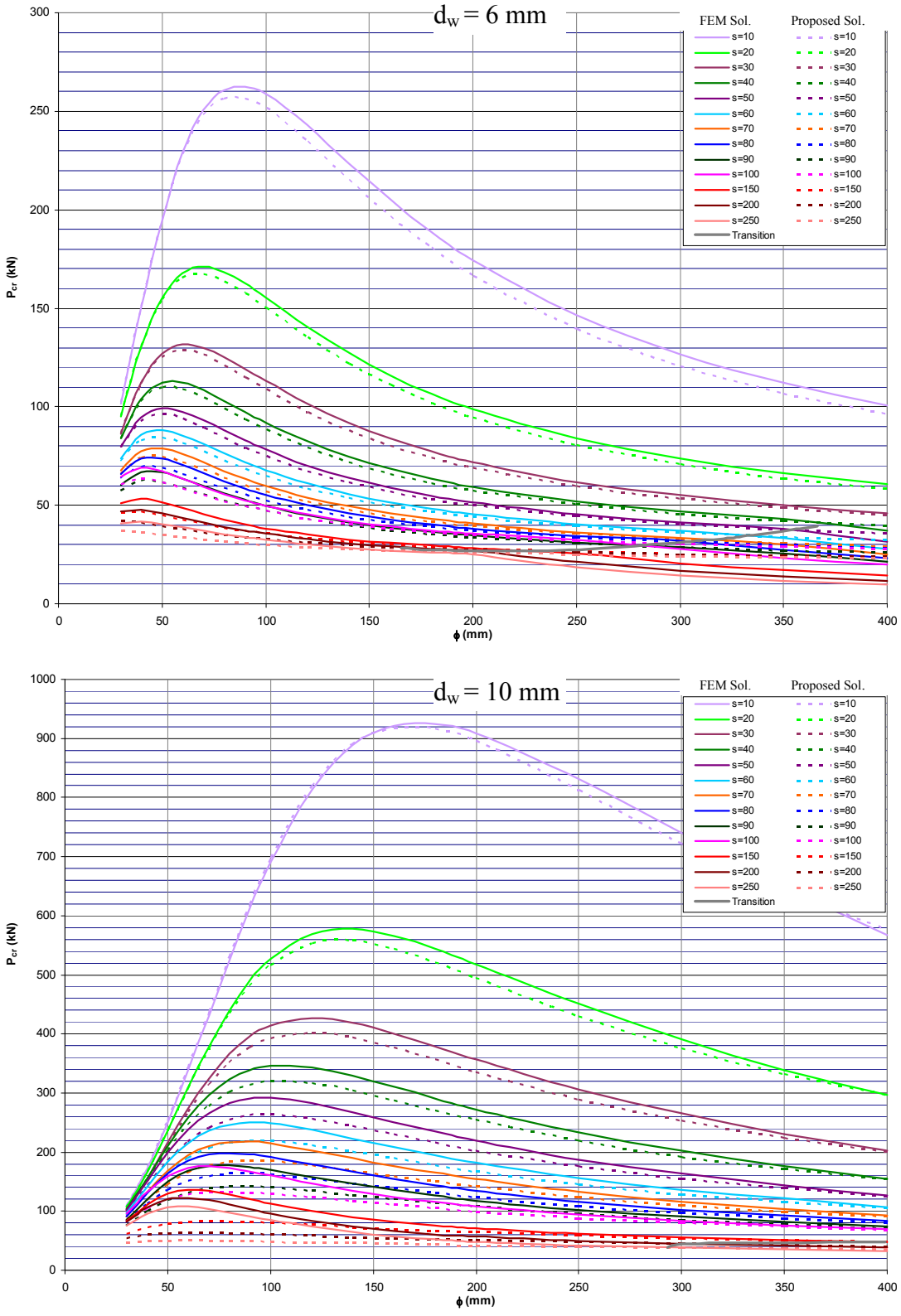

Figure 21 Buckling load of 1000mm members for 25x4mm flange plates

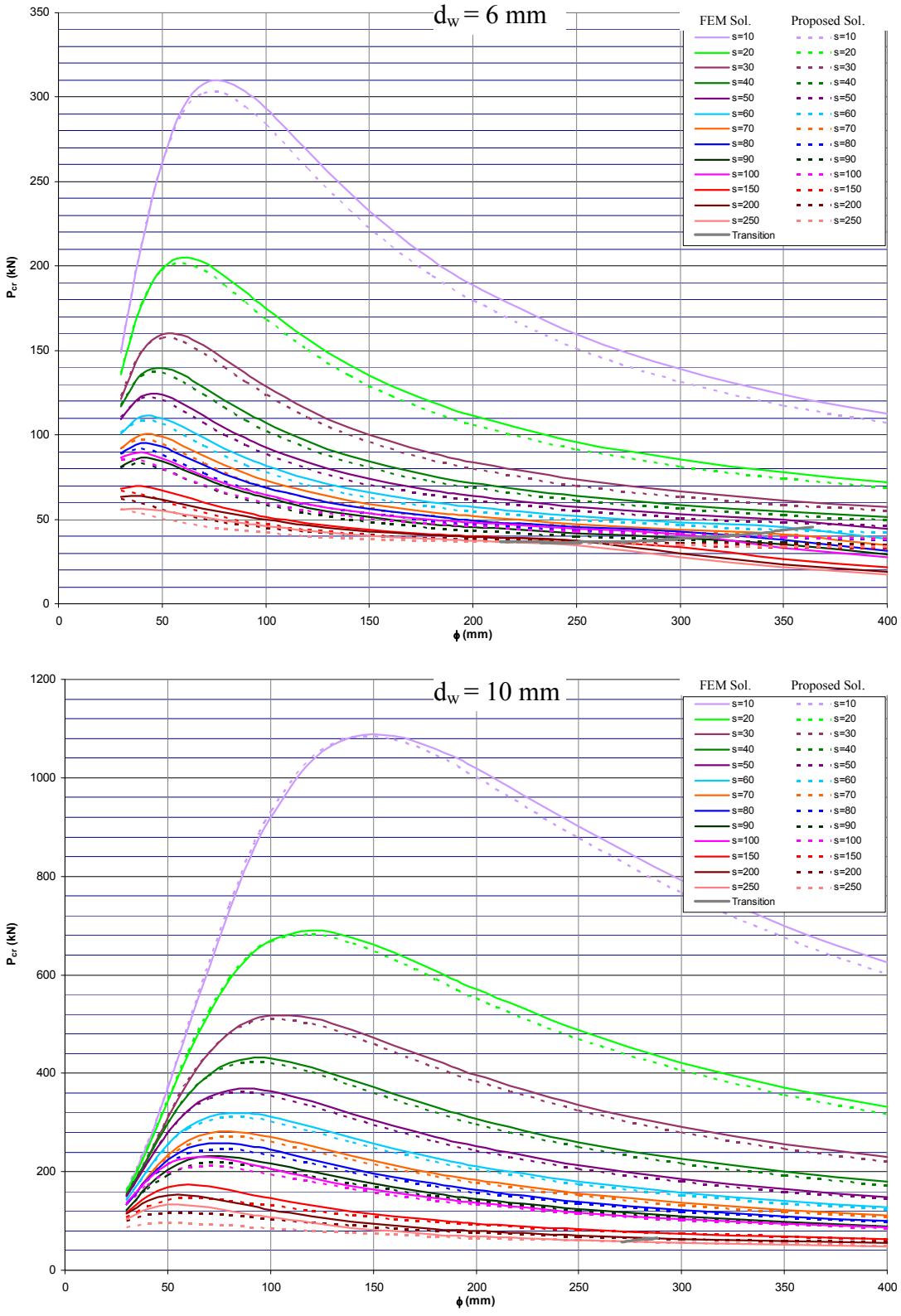

Figure 22 Buckling load of 1000mm members for 25x6mm flange plates

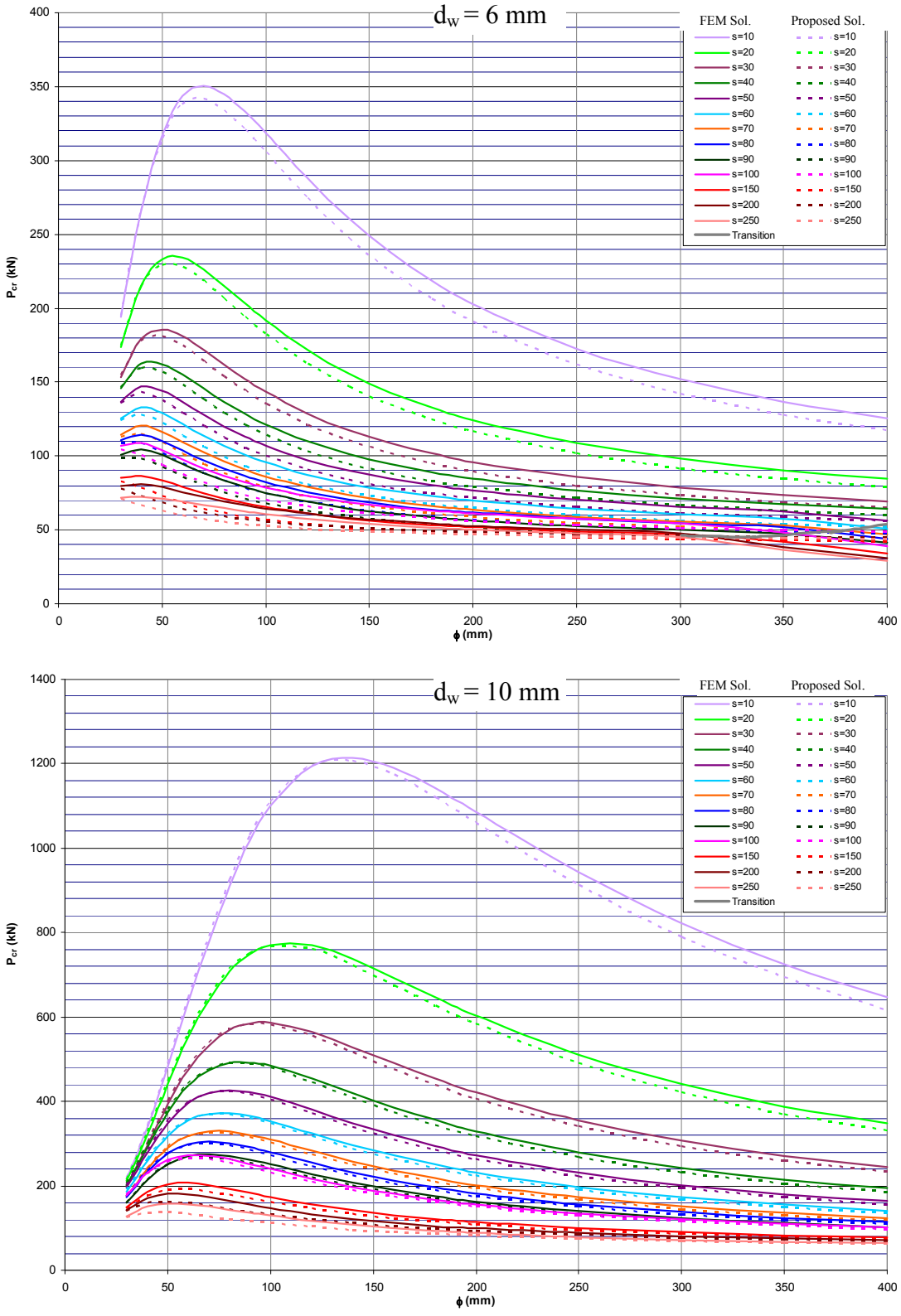

Figure 23 Buckling load of 1000mm members for 25x8mm flange plates

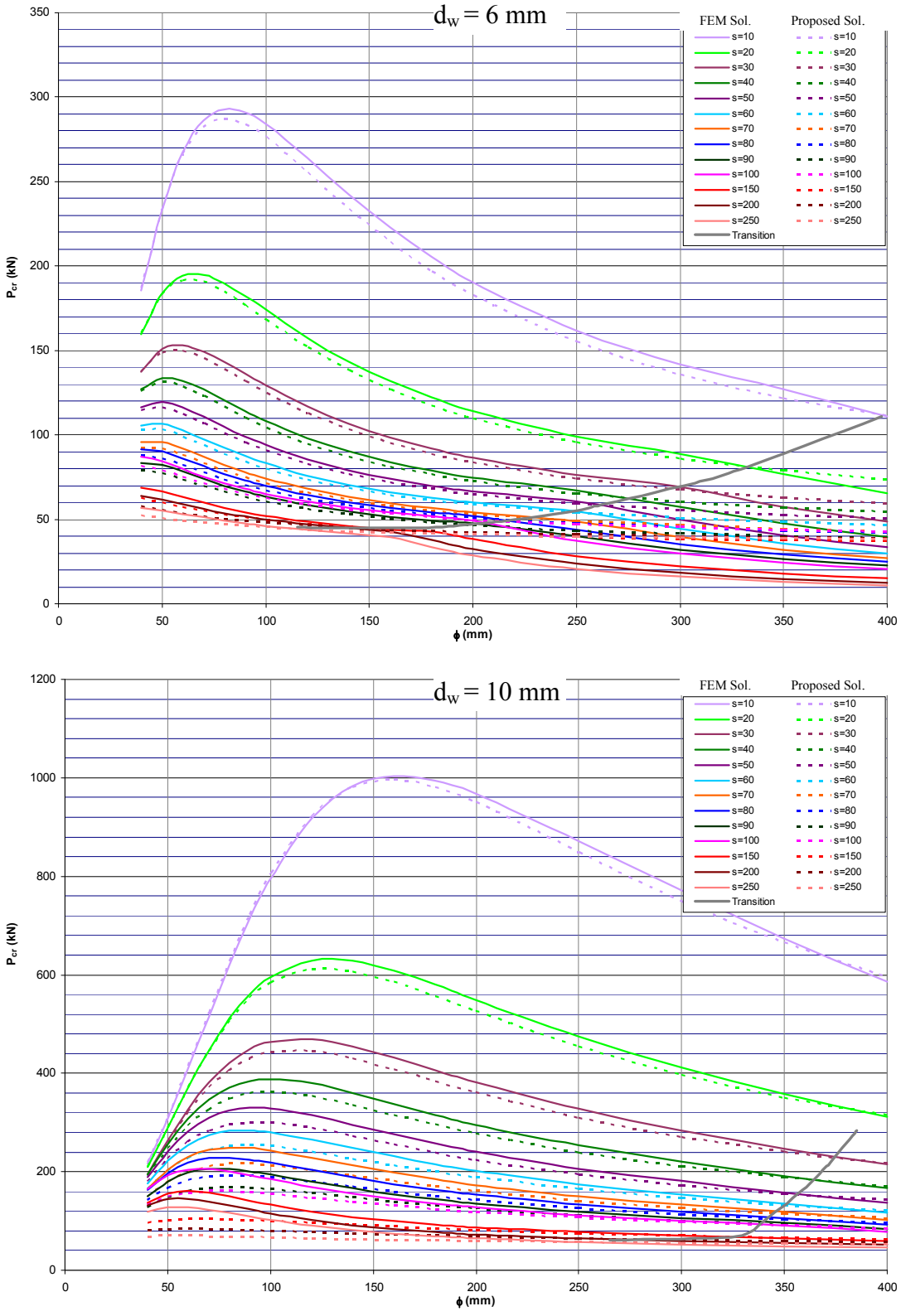

Figure 24 Buckling load of 1000mm members for 30x4mm flange plates

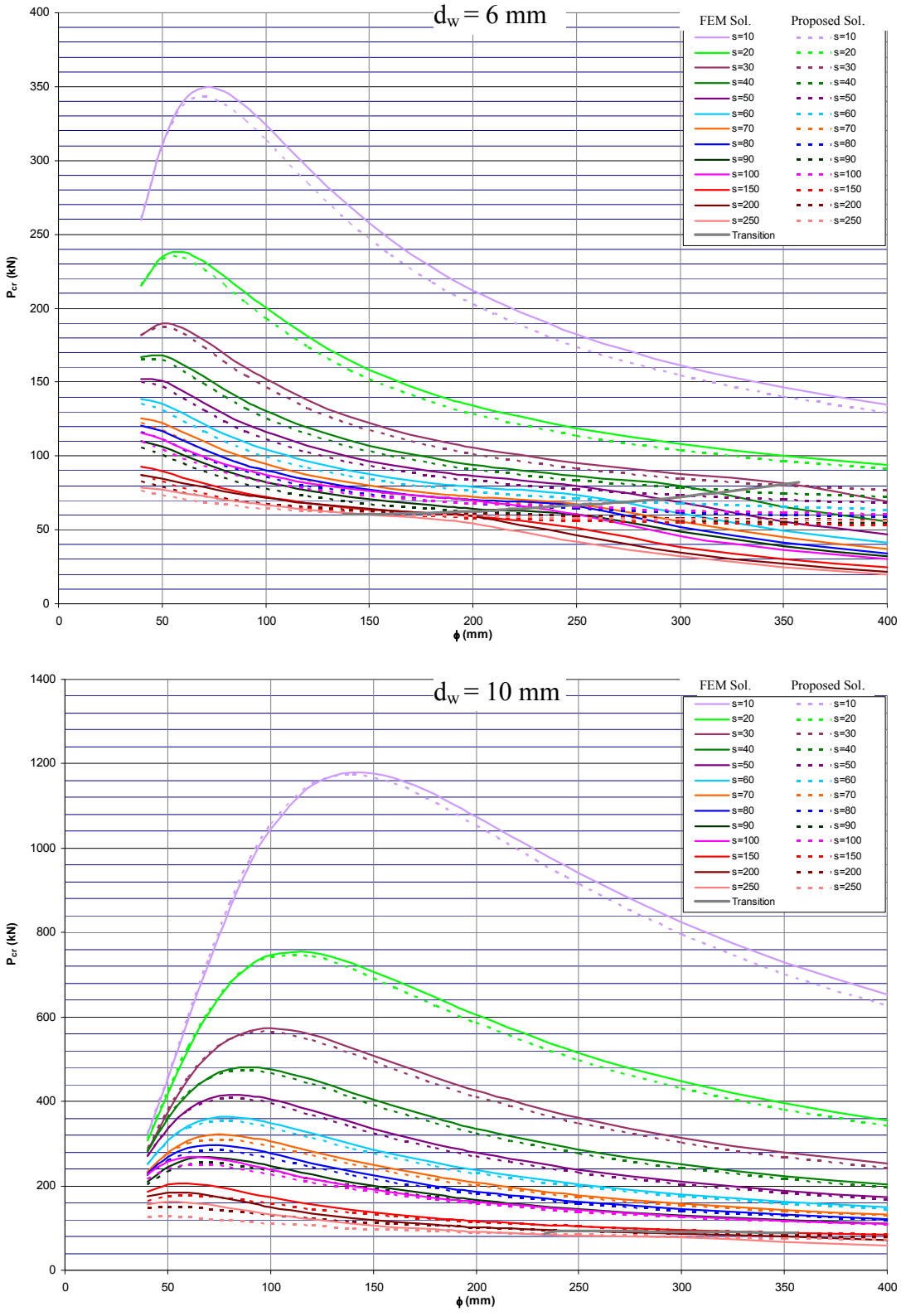

Figure 25 Buckling load of 1000mm members for 30x6mm flange plates

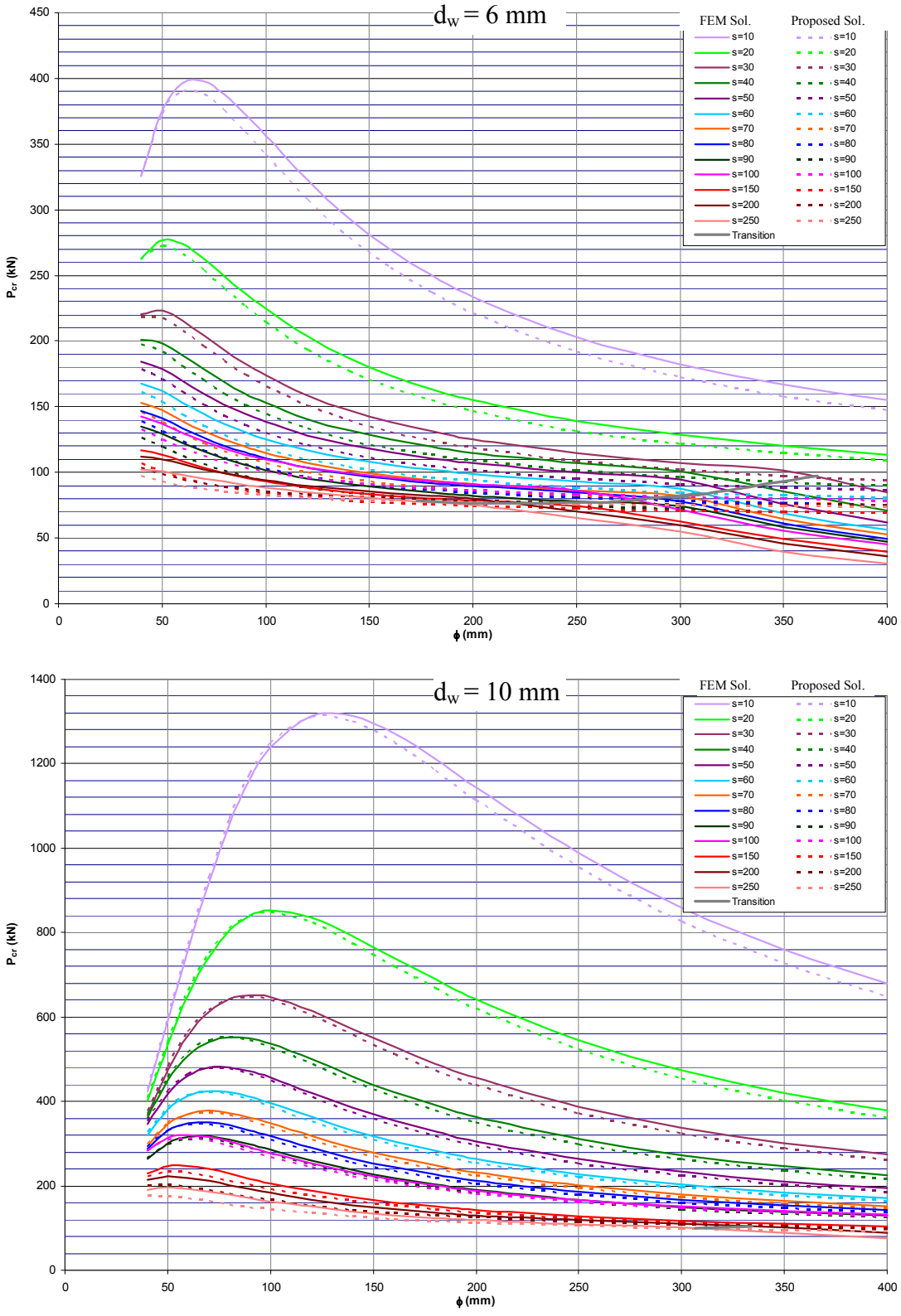

Figure 26 Buckling load of 1000mm members for 30x8mm flange plates

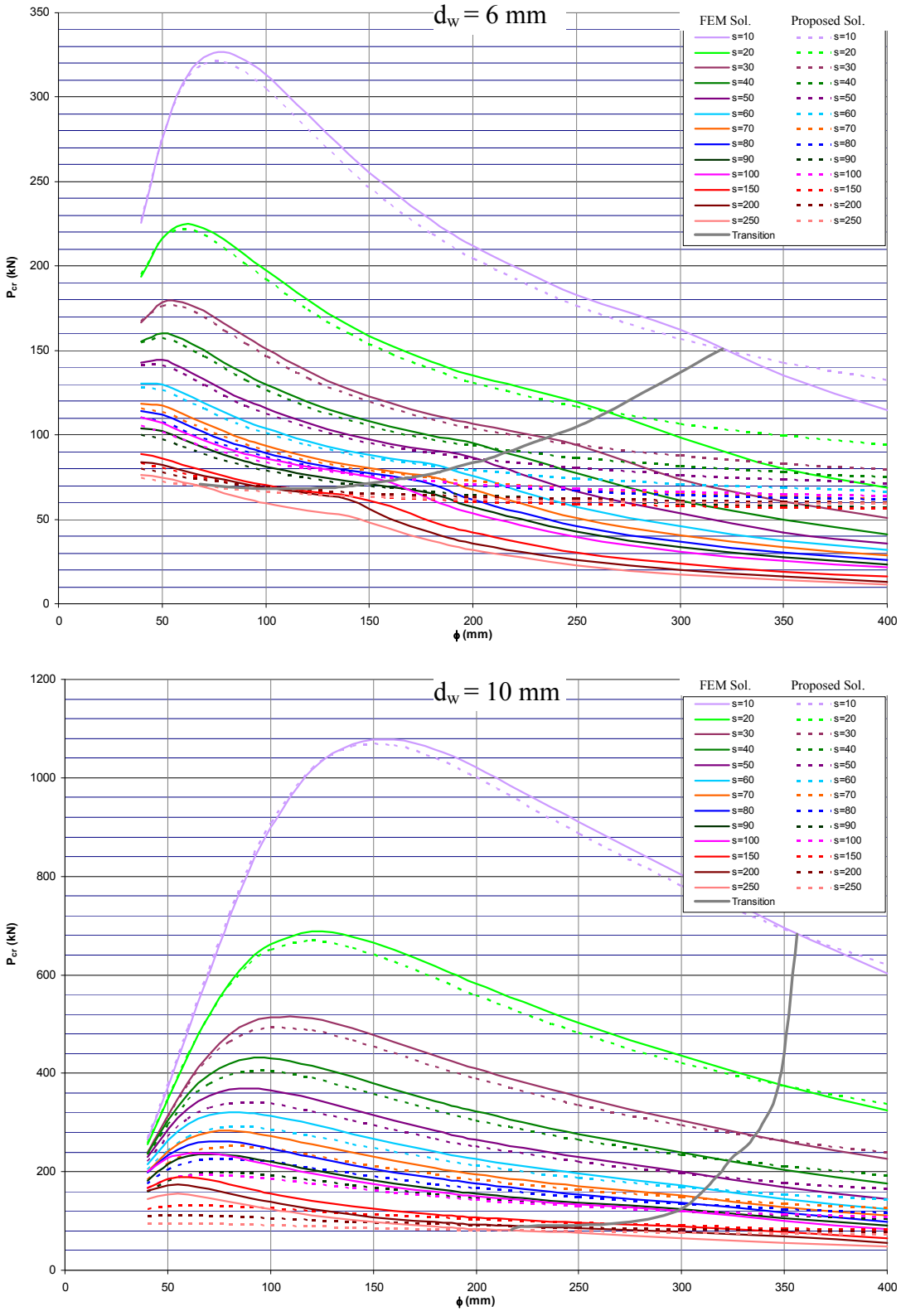

Figure 27 Buckling load of 1000mm members for 35x4mm flange plates

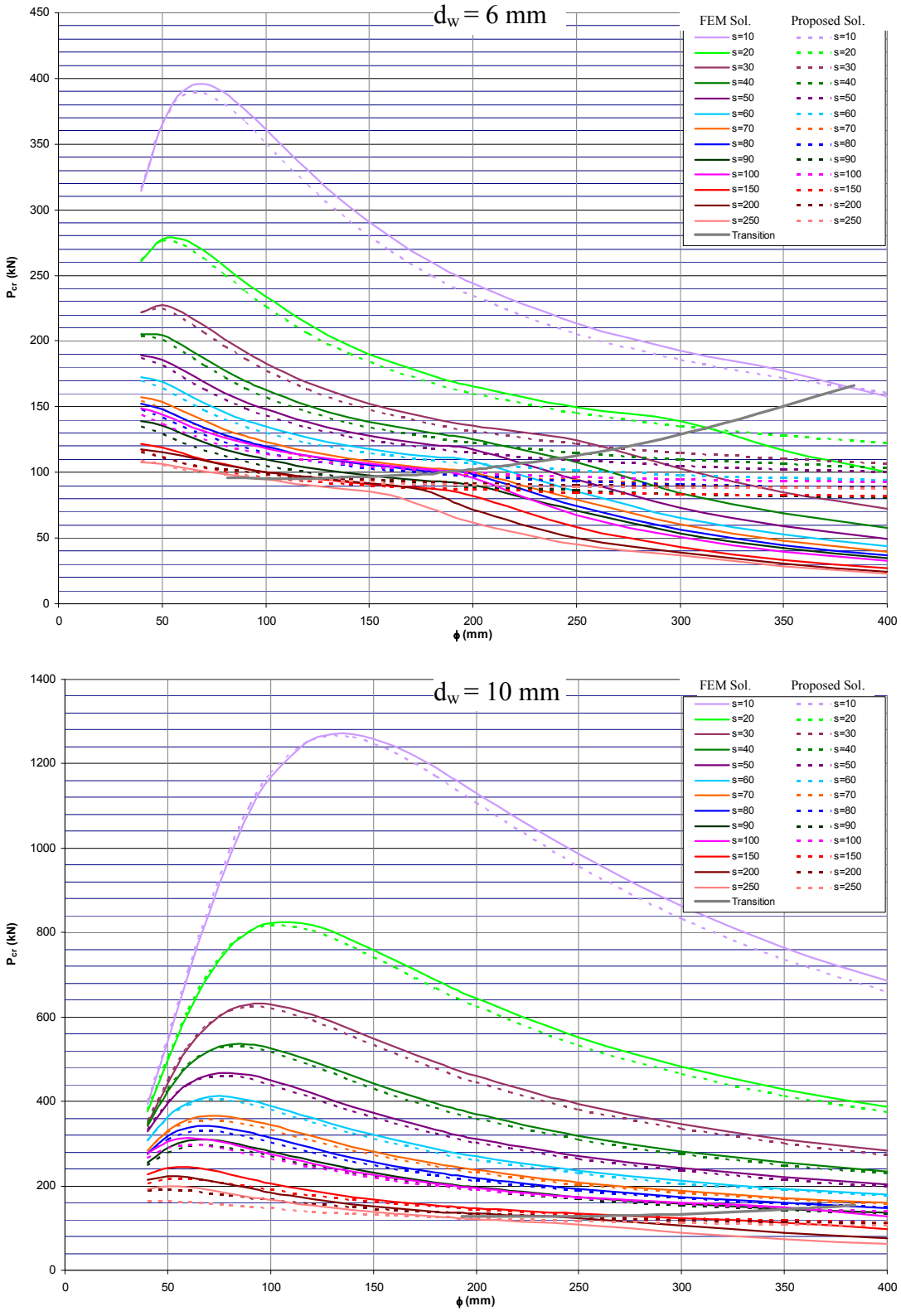

Figure 28 Buckling load of 1000mm members for 35x6mm flange plates

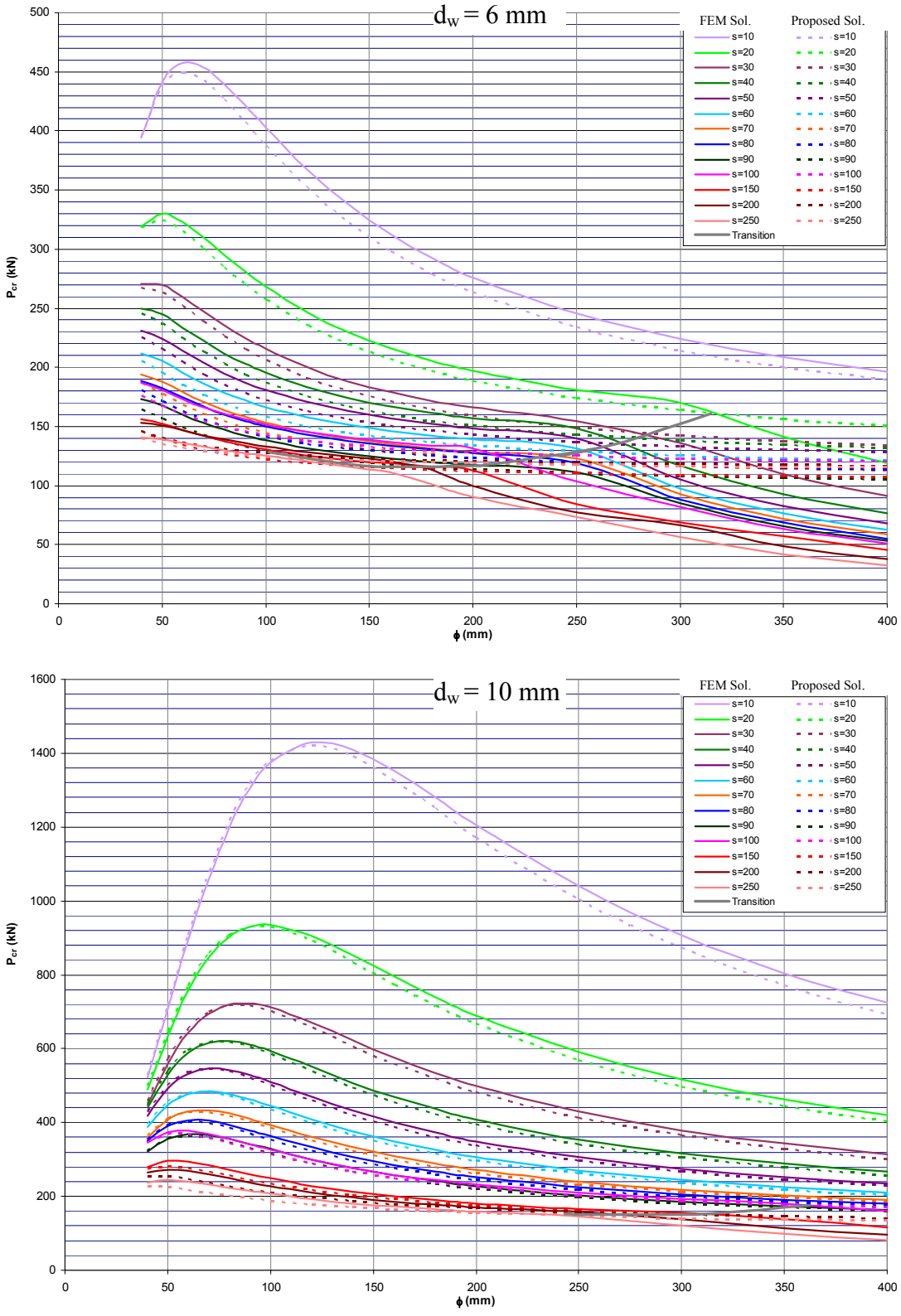

Figure 29 Buckling load of 1000mm members for 35x8mm flange plates

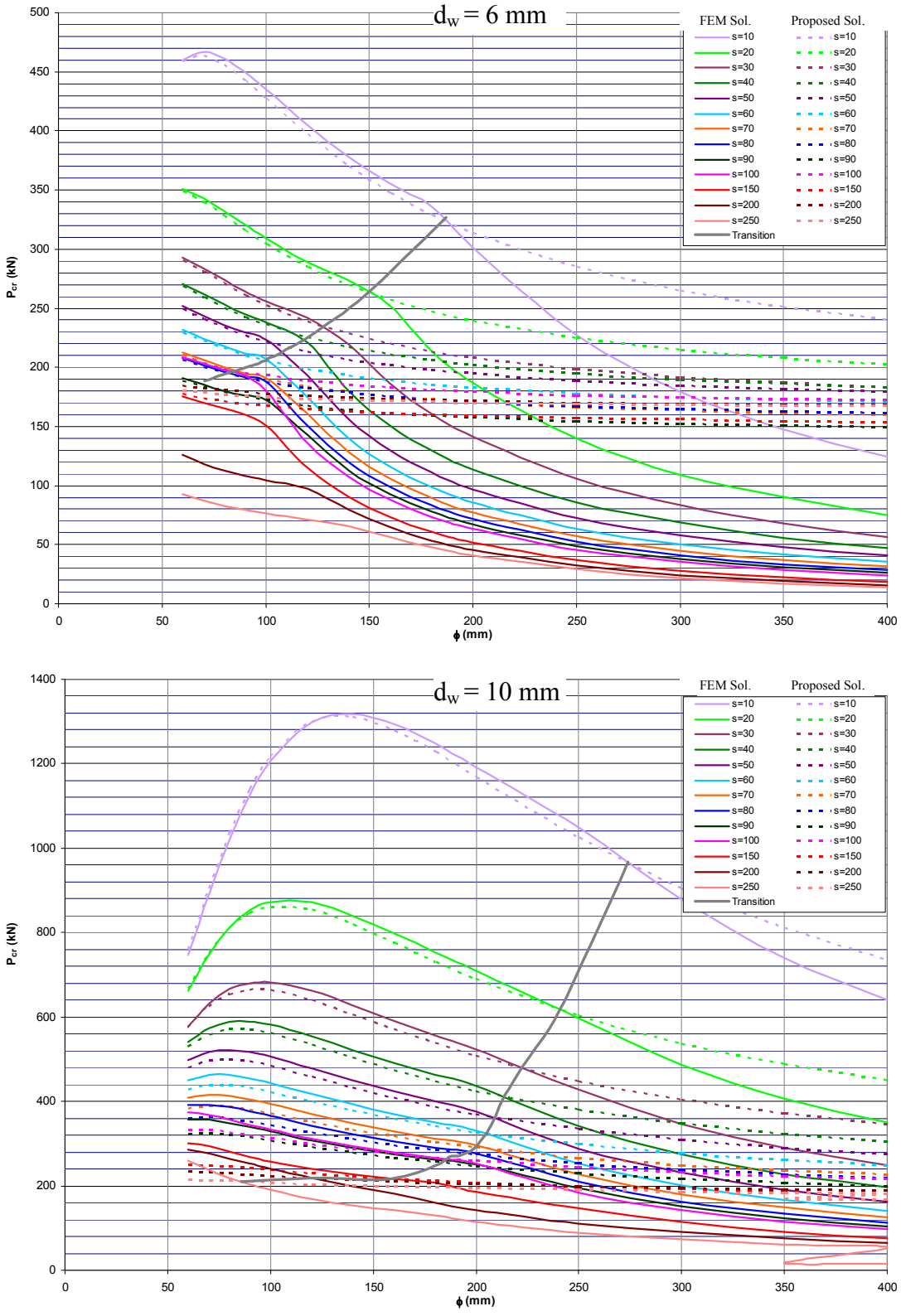

Figure 30 Buckling load of 1000mm members for 50x4mm flange plates

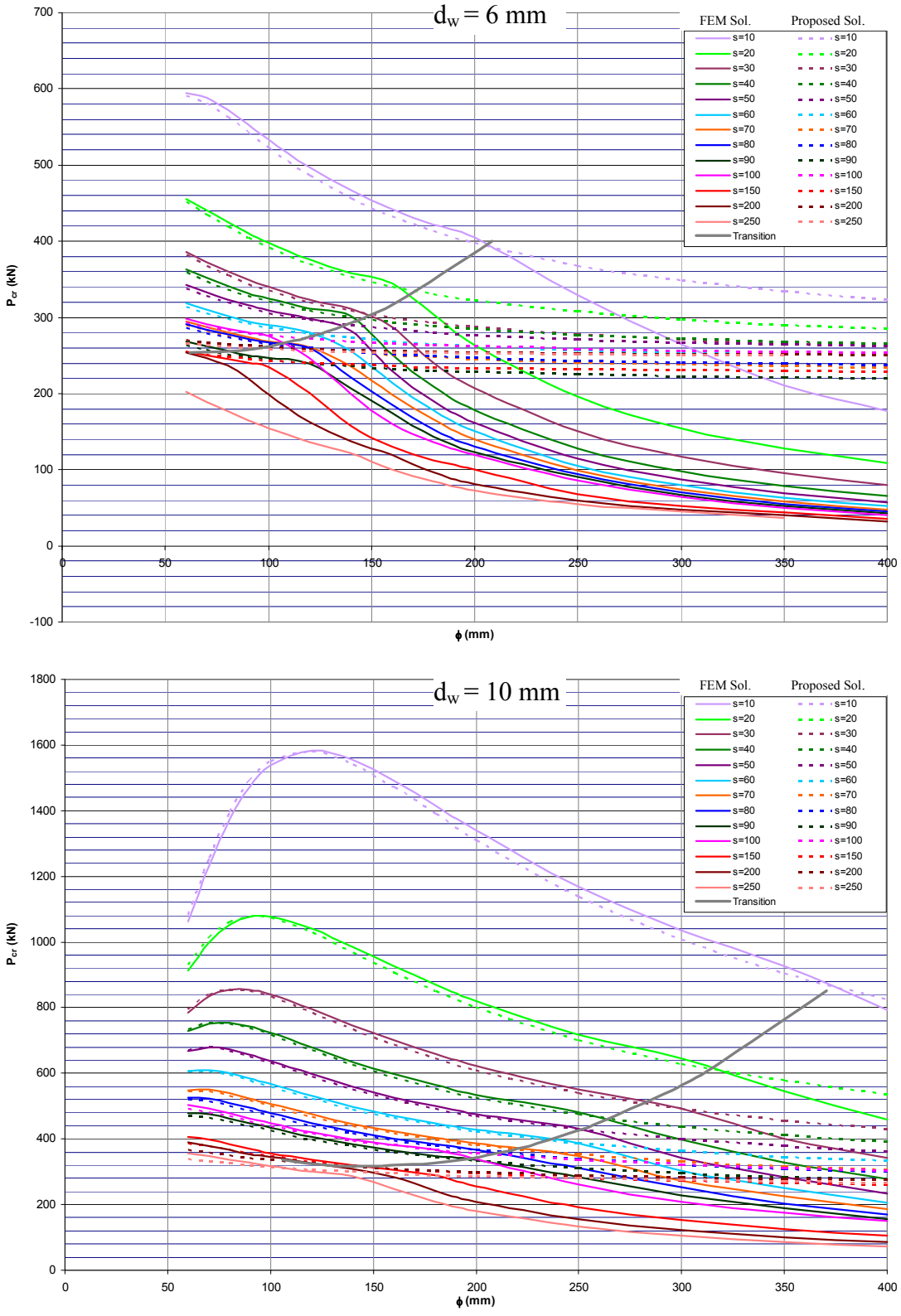

Figure 31 Buckling load of 1000mm members for 50x6mm flange plates

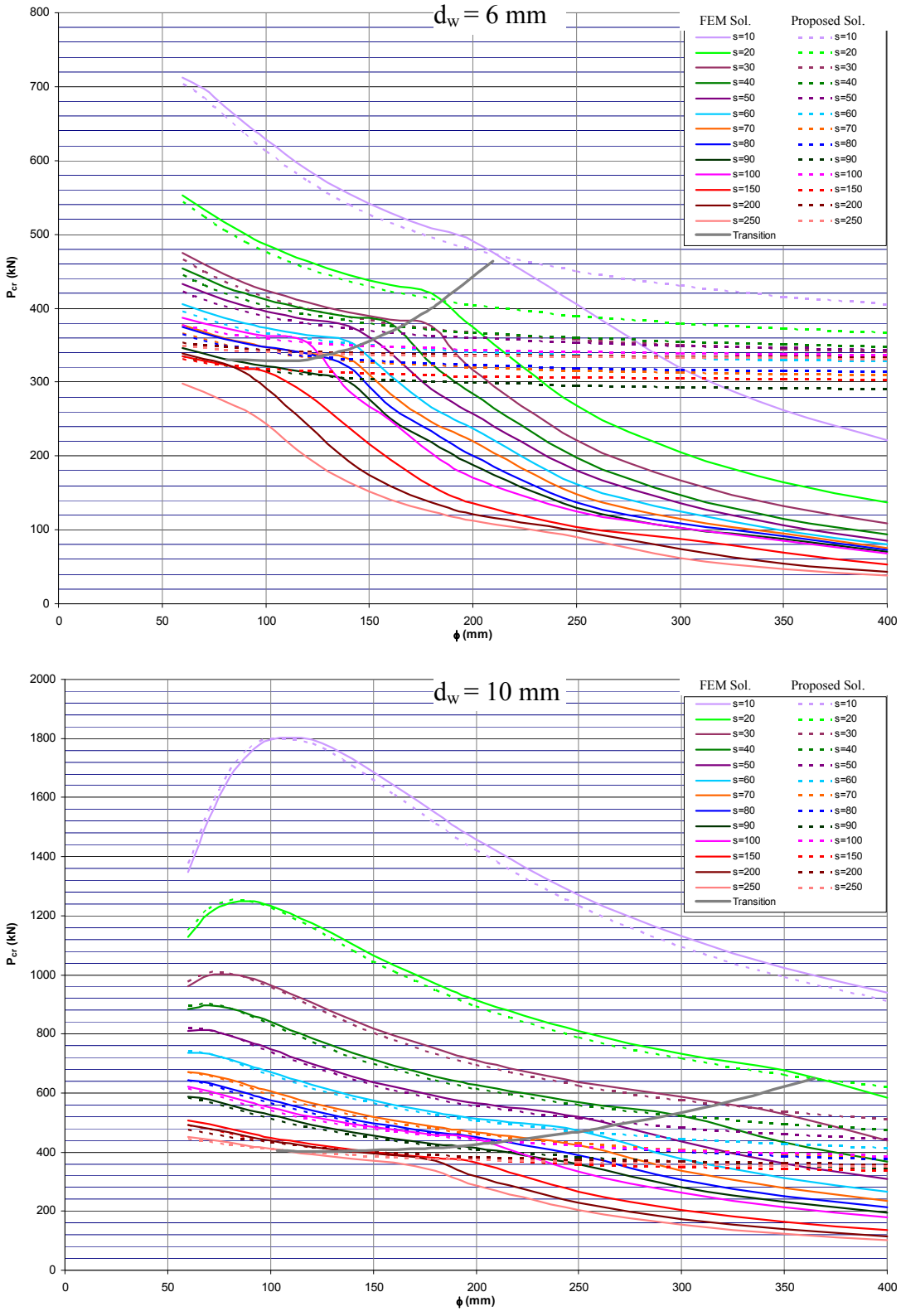

Figure 32 Buckling load of 1000mm members for 50x8mm flange plates

3.5 Correlation of Predictions by Proposed Scheme and FEA

The buckling loads predicted by the finite element analysis are compared with those obtained by the approximate procedure proposed in the previous section. A scatter plot of the buckling loads predicted by the finite element analysis and calculated by the proposed approximate scheme of Section 3.3 for the entire 10530 element models of Section 3.4 are given in Figure 33. It is observed that there is a very acceptable correlation between the two predictions for members with high bearing capacities. However, a large scatter is observed for lower bearing capacities. It is realized that the reason for this scatter is the relative unbalance between the parametric values of a given member such as a helical core pitch much larger than the core diameter or a thin and wide flange plate dimensions. Such combinations of the element parametric values activate buckling modes other than the flexural global mode presumed by the proposed approximate scheme.

Therefore, it is decided to place some restrictions on the wire core diameter, the helical core pitch relative to core diameter and the aspect ratio of the flange plate sections. Consequently, the following constraints are defined and imposed on the parametric combinations to be used by wire core members for whom the proposed approximate scheme is used to calculate its buckling load under compression:

$$\text{Diameter: } 60 \le \phi(\text{helical core diameter}) \le 200 \text{ mm} \tag{3.25}$$

$$\text{Pitch to core diameter ratio: } \frac{\text{S (pitch)}}{\phi \text{ (core diameter)}} \le 0.5 \tag{3.26}$$

$$\text{Flange plate aspect ratio: } \frac{b_f \text{ (flange plate width)}}{t_f \text{ (flange plate thickness)}} \le 5 \tag{3.27}$$

The correlation between the predictions by the finite element analysis and the proposed scheme after successive imposition of the constraints defined in Equations (3.25) - (3.27) are shown in Figure 34, Figure 35 and Figure 36.

A partial list of the calculation steps and the results for a representative range of parameters is also given in Table 2. It is clearly seen that the two predictions are reasonably close.

Table 2 Buckling loads predicted by the approximate procedure and FE Analysis

ϕ (mm)	s (mm)	b (mm)	t (mm)	d (mm)	I_{side} (3.7) (mm^4)	$P_{cr(side)}$ (3.6) (N)	I_{wire} (3.24) (mm^4)	I_{flange} (3.23) (mm^4)	$1/S_v$ (3.22) ($1/Nmm^2$)	S_v (Nmm^2)	$I_{sandwich}$ (3.16) (mm^4)	$N_{cr(teo)}$ (3.15) (N)	P_{cr} (3.5) (kN)	SAP2000 results (kN)	Error
60	20	20	4	6	5333.3	10527.6	63.6	106.7	4.125E-06	242420.5	144213.3	284665.7	141.5	143.5	1.42%
60	30	25	6	6	15625.0	30842.5	63.6	450.0	5.999E-06	166700.2	270900.0	534735.2	157.9	159.0	0.68%
60	30	30	6	8	27000.0	53295.9	201.1	540.0	1.952E-06	512320.7	325080.0	641682.2	338.2	331.3	-2.04%
60	30	35	6	8	42875.0	84631.9	201.1	630.0	1.940E-06	515596.3	379260.0	748629.2	389.9	381.7	-2.11%
60	30	50	8	10	166666.7	328986.8	490.9	2133.3	7.859E-07	1272400.0	724266.7	1429645.1	1002.2	960.9	-4.12%
90	20	20	4	6	5333.3	10527.6	63.6	106.7	6.090E-06	164205.2	324213.3	639971.5	141.2	145.8	3.27%
90	30	25	6	6	15625.0	30842.5	63.6	450.0	8.946E-06	111780.5	608400.0	1200933.5	133.1	136.7	2.66%
90	30	30	6	8	27000.0	53295.9	201.1	540.0	2.884E-06	346686.4	730080.0	1441120.2	332.8	335.2	0.74%
90	40	35	8	8	57166.7	112842.5	201.1	1493.3	3.786E-06	264131.2	1136986.7	2244321.7	349.2	358.9	2.79%
90	50	50	8	10	166666.7	328986.8	490.9	2133.3	1.971E-06	507383.8	1624266.7	3206173.9	767.0	773.0	0.78%
120	20	20	4	6	5333.3	10527.6	63.6	106.7	8.055E-06	124149.3	576213.3	1137399.5	122.5	127.5	4.15%
120	30	25	6	6	15625.0	30842.5	63.6	450.0	1.189E-05	84080.1	1080900.0	2133611.1	111.7	115.3	3.22%
120	40	30	6	8	27000.0	53295.9	201.1	540.0	5.128E-06	195011.1	1297080.0	2560333.3	234.5	241.8	3.13%
120	50	35	6	8	42875.0	84631.9	201.1	630.0	6.424E-06	155674.3	1513260.0	2987055.5	232.6	239.2	2.84%
120	60	50	8	10	166666.7	328986.8	490.9	2133.3	3.144E-06	318100.0	2884266.7	5693314.2	630.3	626.8	-0.55%
200	50	20	4	6	5333.3	10527.6	63.6	106.7	3.397E-05	29438.9	1600213.3	3158694.5	39.7	41.3	4.01%
200	60	25	6	6	15625.0	30842.5	63.6	450.0	3.971E-05	25179.9	3000900.0	5923539.2	55.9	57.2	2.30%
200	70	30	6	8	27000.0	53295.9	201.1	540.0	1.498E-05	66760.5	3601080.0	7108247.0	119.4	118.1	-1.11%
200	80	35	8	8	57166.7	112842.5	201.1	1493.3	1.680E-05	59517.2	5602986.7	11059852.4	172.0	169.8	-1.28%
200	100	50	8	10	166666.7	328986.8	490.9	2133.3	8.732E-06	114516.0	8004266.7	15799789.1	442.7	444.9	0.50%

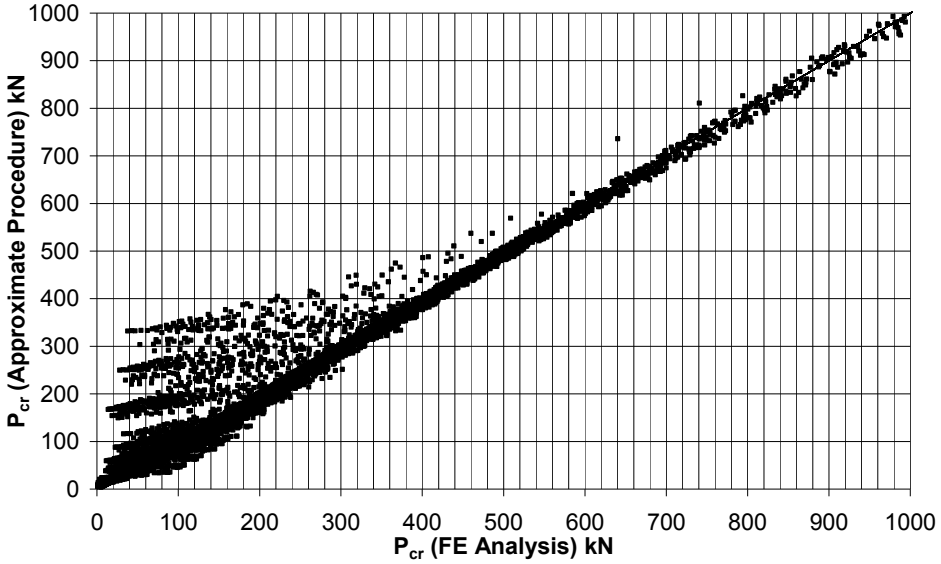

Figure 33 Comparison of the buckling loads without constraints.

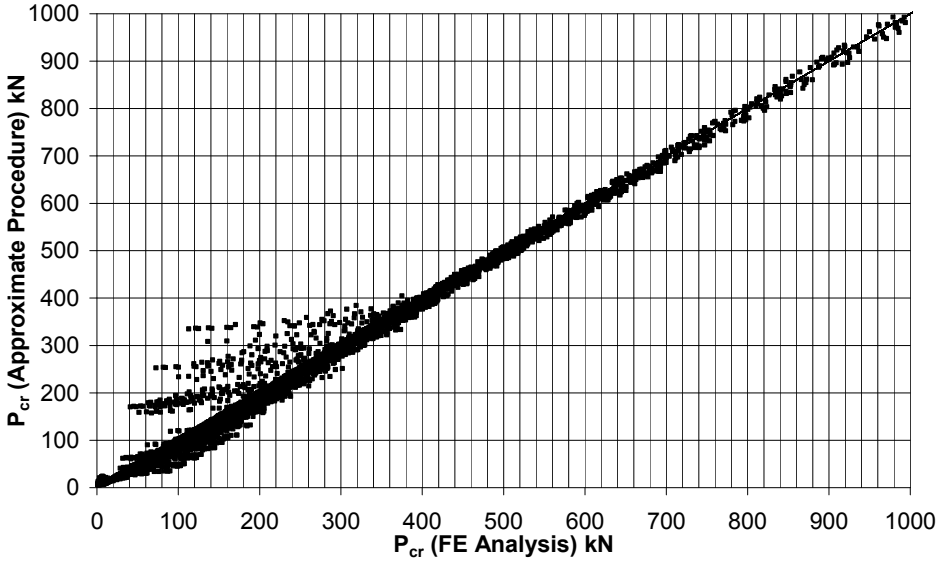

Figure 34 Comparison of the buckling loads estimated by FEM and the approximate procedure after imposing the Diameter constraint

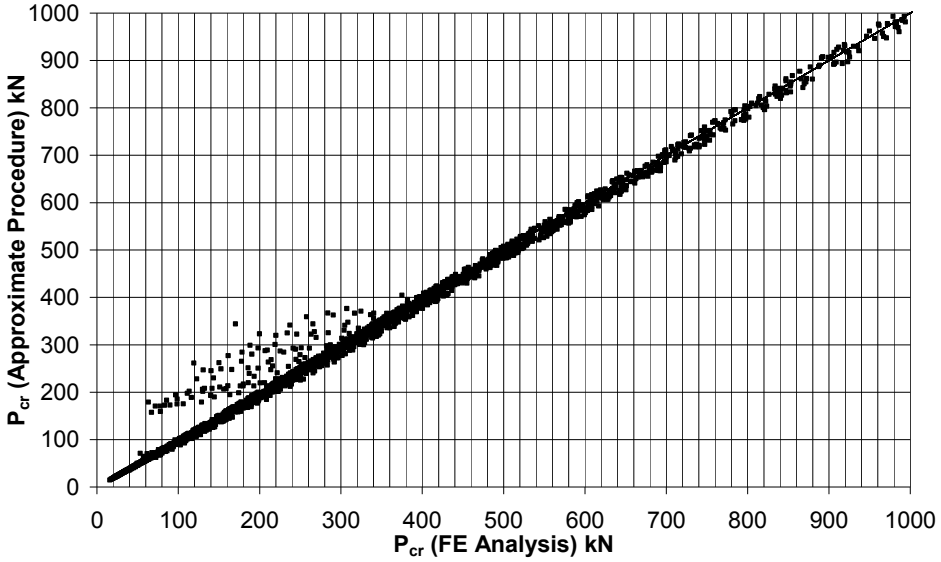

Figure 35 Comparison of the buckling loads estimated by FEM and the approximate procedure after imposing the Diameter and Pitch constraints

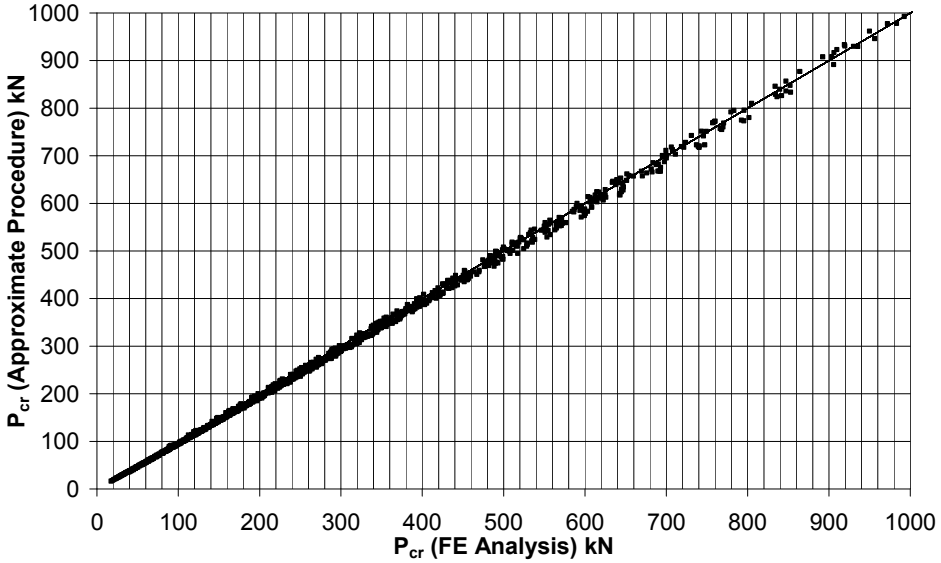

Figure 36 Comparison of the buckling loads estimated by FEM and the approximate procedure after imposing Diameter, Pitch and Aspect Ratio constraints

3.6 Experimental Verification

To check the validity of assumptions and have a global sense of behavior of the members, a limited experimental study is carried out in the Materials of Construction Laboratory in the Department of Civil Engineering at METU. For this purpose, a total of three members are prepared and tested under compression. The specimens are 1.0 m long and each has a different combination of basic parameters. The experimental results are compared with the analytical predictions.

Simply supported end conditions are created for the specimens and the axial load is applied through a relatively rigid end plates. This is to ensure that the applied axial load is distributed equally on the 4 flange plates (Figure 37, Figure 38 and Figure 39). The compressive load is applied from a central point without any restraint to enable rotation at the ends of the member. Hence, the effective length factor for the specimen can be taken as $\lambda = 1$. The specimen parameters together with the test results and analytical predictions are listed below in Table 3.

Table 3 Experimental and theoretical result comparison

Specimen	ϕ (mm)	S (mm)	b_f (mm)	t_f (mm)	d_w (mm)	Theoretical Results (kN)	SAP2000 results (kN)	Yield Capacity (kN)	Experiment Results (kN)	Difference (%)
1	60	30	20	6	6	135.4	136.2	**115.2**	90.4	22%
2	60	30	30	6	6	185.9	186.8	**172.8**	148.2	14%
3	100	100	50	8	6	**359.1**	362.0	384.0	299.2	22%

It is seen that the analytical predictions for the bearing capacity are very close to those predicted numerically by the finite element analysis. However, the test results are somehow lower than the expected. The difference is approximately 20%. This is

because the stress level in each specimen is near the material yield level and it is known that the tangential modulus of elasticity of the material gets lower at this stress level.

The yield capacity column in Table 3 shows the specimen ultimate capacity calculated as follows:

$$\text{Yield Capacity} = \text{Flange plate sectional area} \times \sigma_y = 4b_f t_f \sigma_y \tag{3.28}$$

where $\sigma_y = 240\ \text{MPa}$. Therefore,

$$\text{Yield capacity} = 960 b_f t_f \tag{3.29}$$

The yield capacities of specimens are lower than their expected buckling loads. Hence, the members are expected to yield before they loose their stability for the first two specimens. However, the test results show that this is not the case. This is because the instability of columns at high stress levels close to material yielding is by inelastic buckling, and the modulus of elasticity E in Euler's formula must reflect this softening in material response. Therefore, the Euler's buckling formula, derived for materials following Hooke's law, can also be used for inelastic materials by substituting the reduced modulus E_r for the modulus of elasticity E.

$$P_{cr} = \frac{\pi^2 E_r I}{L_{eff}^{\ 2}} \tag{3.30}$$

In Table 3 the experimental results are about 20% lower than the expected values. This corresponds to a reduction of 20% in the effective modulus of elasticity of steel at this level of stressing which is very reasonable.

Figure 37 Specimen 1: ϕ60-s30-20x6 bearing capacity: 90.4 kN

Figure 38 Specimen 2: ϕ60-s30-30x6 bearing capacity: 148.2 kN

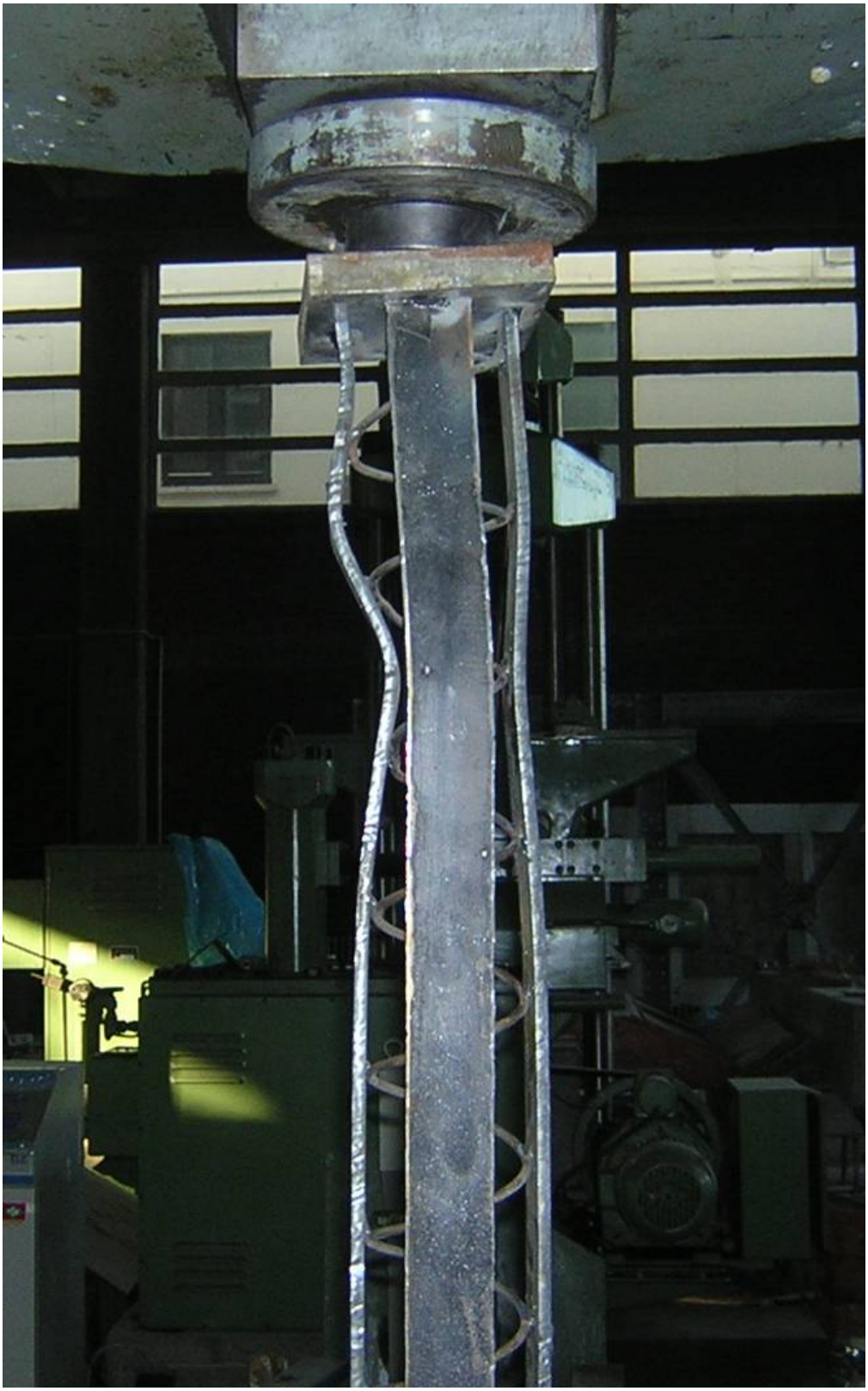

Figure 39 Specimen 3: ϕ100-s100-50x8 bearing capacity: 299.2 kN

3.7 Validity of Modeling Assumption

The modeling of the member was made by ignoring the eccentricity at the junctions of the flange plates and the wire core for simplicity. In the analysis models the wire axis of the core is assumed to be coincident with that of the flange plates at their intersections. However there is actually a distance of $(d_w + t_f) / 2$ between them. This simplification results in a reduction in the buckling load capacities of the members predicted by the analysis models. A better mathematical model would be created by using rigid links between the flange plates and the helical core wire at the junctions. (See Figure 40)

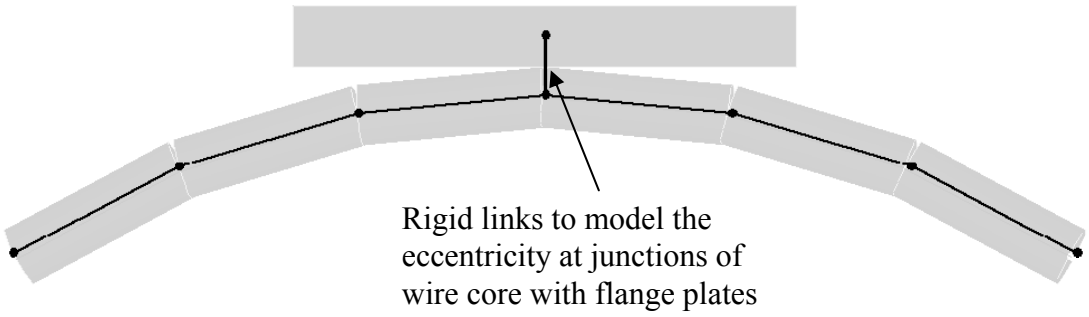

Figure 40 Modeling with rigid links

The buckling load predictions by using of finite element models with eccentric and concentric connections are given in Table 4 for helical wire core members with a small and a large diameter for comparison. It is seen that the error introduced into the predicted buckling loads of the members due to ignoring this eccentricity at the junctions is more pronounced for members with smaller diameters.

Table 4 Buckling load predictions by eccentric and concentric connection models

ϕ (mm)	s (mm)	b (mm)	t (mm)	d (mm)	L (mm)	Proposed method (kN)	SAP2000 w/o rigid links (kN)	SAP2000 w/ rigid links (kN)	Error
60	30	30	6	6	1000	185.9	186.8	264.0	41.55%
200	50	50	6	6	2000	91.8	94.1	100.5	6.97%

3.8 Feasibility Study

The study is focused on the structural bearing capacity of helical wire core truss members under axial compression. In order to have an idea about the economic effectiveness of such members, a limited feasibility study is carried out comparing the bearing capacity of these members with those of cylindrical pipes with an equivalent sectional area. For this purpose the buckling load capacities are calculated for some commercially available and commonly used pipe sections. The results are listed in Table 5, below.

Table 5 Buckling loads for some standard pipe sections

Section	Outside Diameter (mm)	Thickness (mm)	Internal Diameter (mm)	Moment of Inertia (mm^4)	Sectional Area (mm^2)	Bearing Capacity	
						L=2000mm (kN)	L=6000mm (kN)
1	60.3	3.65	53.0	261669	649.59	129.13	14.35
2	88.9	5.50	77.9	1258361	1441.05	620.98	69.00
3	114.3	6.00	102.3	3002116	2041.41	1481.48	164.61
4	165.2	6.00	153.2	9520434	3000.85	4698.15	522.02

In the following figures, Figure 41–Figure 44, the buckling load capacities of the pipe sections listed in Table 5 are compared with various helical wire core truss member configurations having the same cross-sectional area as the pipe sections. For simplicity, the wire diameter is taken as d_w=8 mm for the wire core truss members. Neglecting the weight of the wire core it is seen that the wire core truss members can be an economic alternative for small diameter pipes. However, as the diameter increases the commercial pipe sections have higher capacities than helical core truss members. It is also seen that the helical wire core members become more economical as the element length increases.

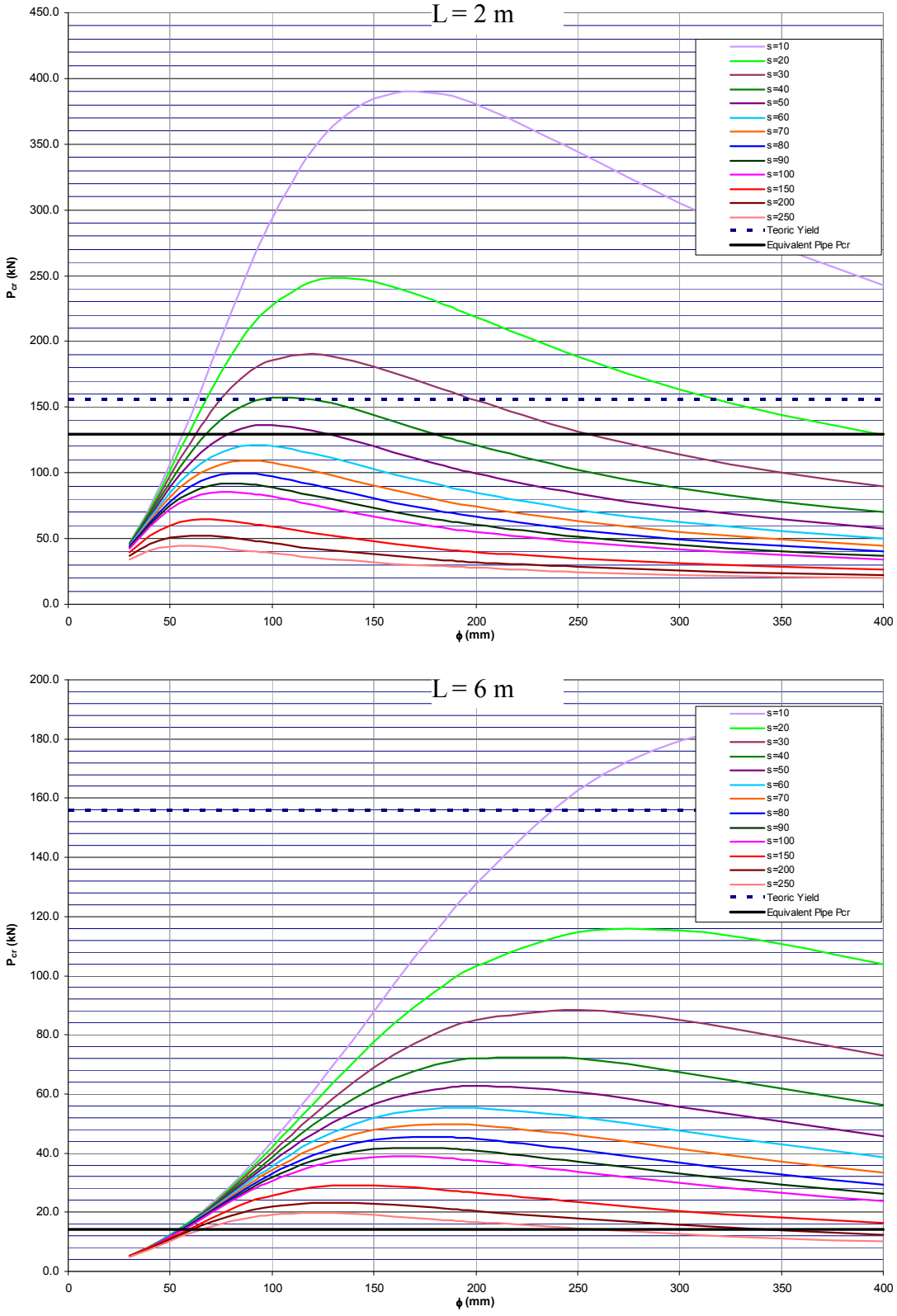

Figure 41 Buckling loads for pipe section #1 and equivalent wire core members

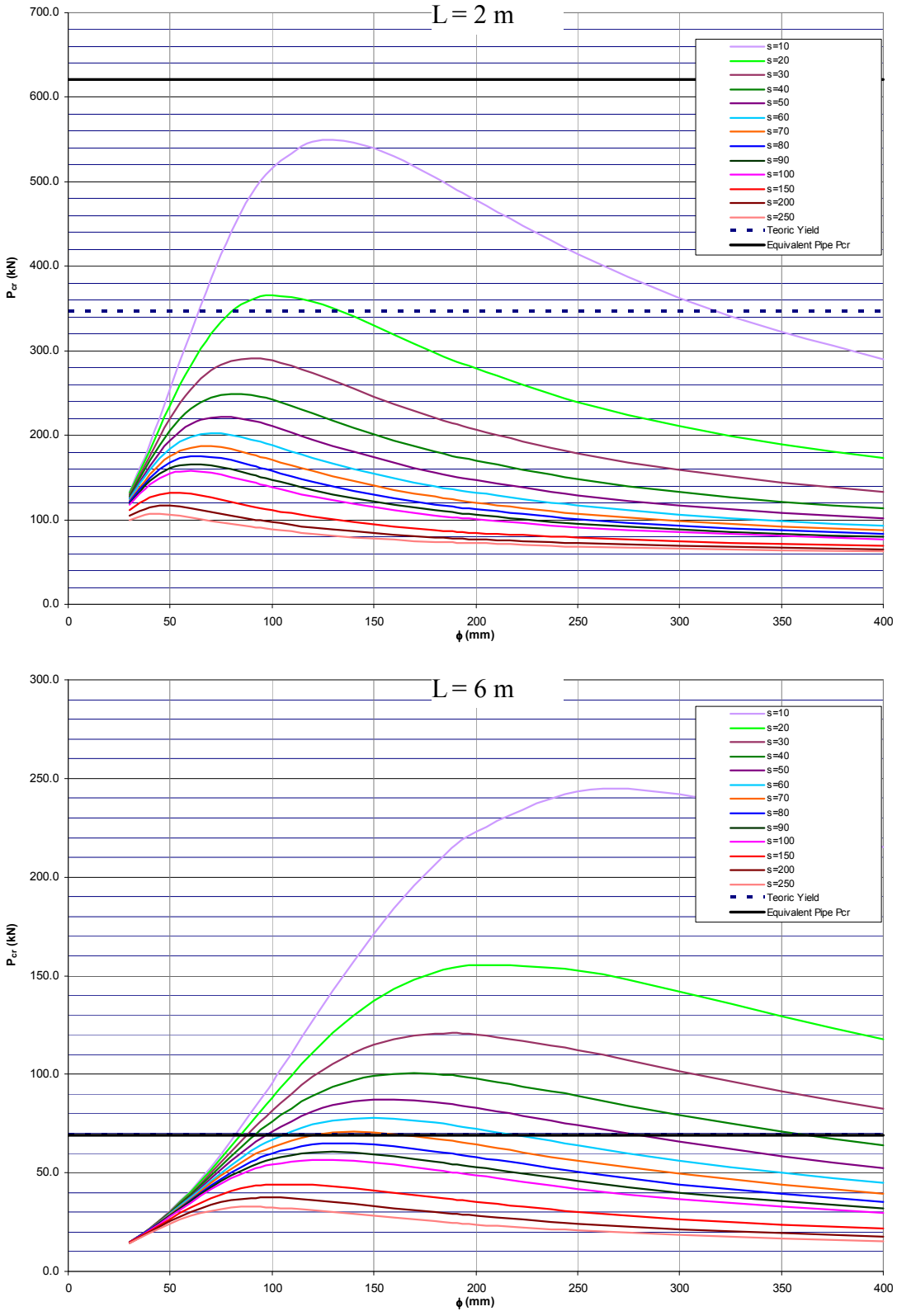

Figure 42 Buckling loads for pipe section #2 and equivalent wire core members

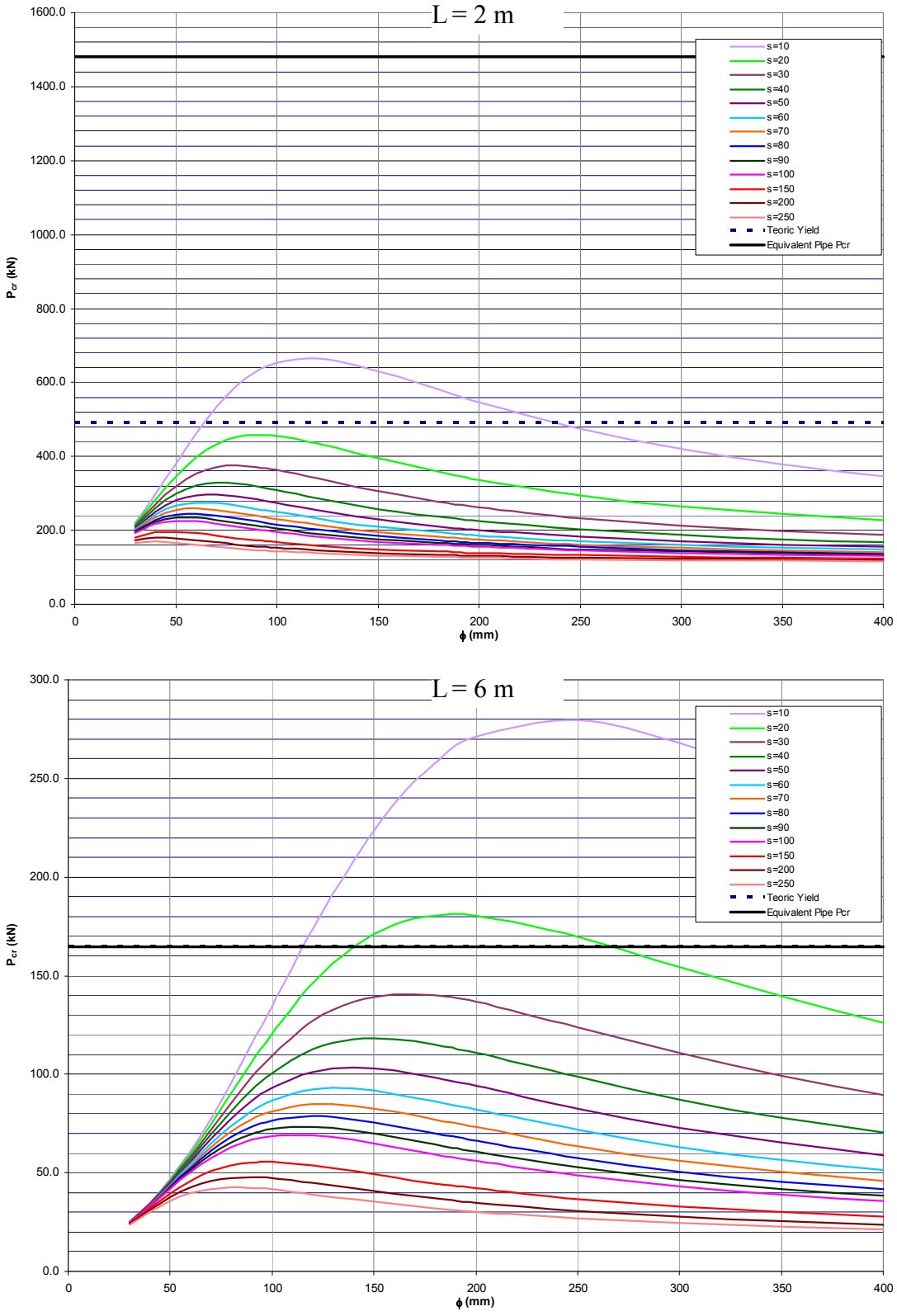

Figure 43 Buckling loads for pipe section #3 and equivalent wire core members

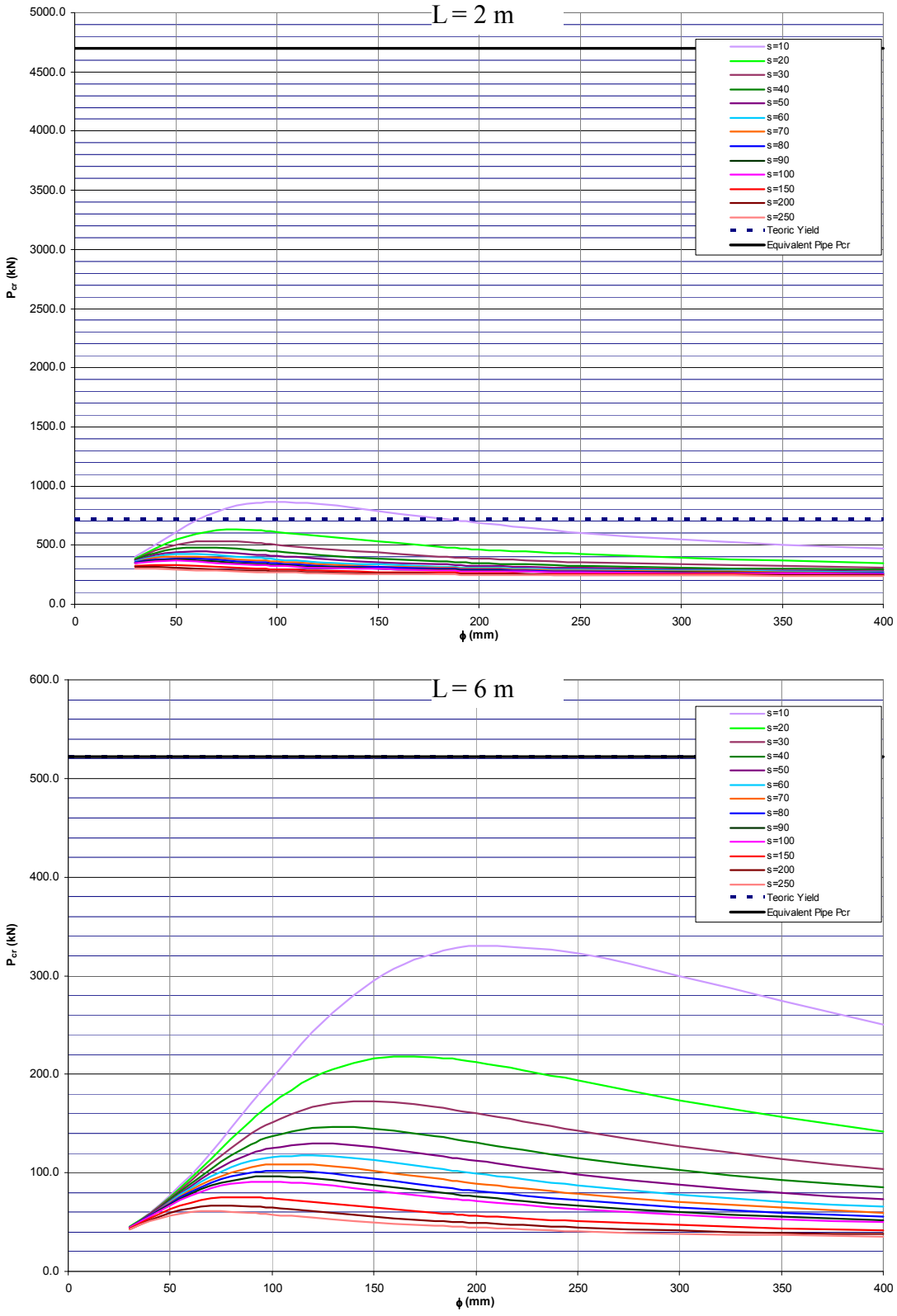

Figure 44 Buckling loads for pipe section #4 and equivalent wire core members

CHAPTER 4

SUMMARY AND CONCLUSION

In the present study, the behavior of three-dimensional helical wire core truss member under compression is studied. An interface, which allows the user define the related model parameter, was programmed in Visual Basic and used to develop and analyze the mathematical models of many cases with the commercial finite element analysis software SAP2000 [27]. Several analyses results have shown that the bearing capacity of a helical wire core truss member is largely affected by the shear deformations. Hence, analyzing helical wire core truss members without proper representation of the shear deformations may lead to severe errors and unconservative results.

The reduction in the bearing capacity of axially loaded members as a result of shear deformations is a well-known issue in engineering and it is a major problem for sandwich beams and built-up columns. A procedure is proposed in Eurocode 3 [28] for the calculation of the critical loads of built-up columns under axial compression. Using a similar procedure, the behavior of the helical wire core truss members was studied and satisfactory results were obtained.

When the critical bearing capacity of a helical wire core truss members under axial compression is studied, it is observed that there are basically three possible modes of failure:

1. Flexural global buckling

2. Flexural local buckling

3. Torsional global buckling

Flexural global buckling is the dominant mode of failure for helical wire core truss members having practical and reasonable combinations of the basic parameters. However, as the flanges get stiffer or the core diameter and pitch increases, the failure mode tends to be torsional global buckling or flexural local buckling. Therefore, in the prediction of the bearing capacity of a helical wire core truss member the possibility of instability by flexural local or torsional global buckling must be taken into consideration.

The ultimate bearing capacities of wire core truss members with different combinations of the basic parameters based on the flexural global buckling are derived and presented in a graphical form. The sensitivity of the bearing capacities to each parameter can easily be seen from these graphs. The transition boundaries from flexural global buckling into flexural local or torsional buckling can also be seen in these graphs.

In general, shear lag between the flange plates results in a loss of bearing capacity of the members. Based on the finite element analysis results, it is evident that as the spiral pitch gets smaller, the shear lag diminishes which, in turn, results in an increase in the ultimate bearing capacity of the member.

It is also evident that when the core diameter increases, the shear lag increases. Therefore, the increase in bearing capacity is not directly proportional to the core diameter. Part of the capacity gain due to an increase in sectional inertia is offset by the loss in capacity due to shear lag.

In order to restrict the basic mode of instability to flexural global buckling and prevent the transition into torsional global or flexural local buckling, the following approximate constraints are proposed based on the results obtained in the numerical analysis of the helical wire core truss member:

$$\text{Diameter: } 60 \le \phi(\text{helical core diameter}) \le 200\,\text{mm} \tag{3.25}$$

$$\text{Pitch to core diameter ratio: } \frac{\text{S (pitch)}}{\phi\ \text{(core diameter)}} \leq 0.5 \tag{3.26}$$

$$\text{Flange plate aspect ratio: } \frac{b_f\ \text{(flange plate width)}}{t_f\ \text{(flange plate thickness)}} \leq 5 \tag{3.27}$$

The study addresses the flexural global buckling of helical wire core truss members which are straight and has a length of 1000 mm or longer. The basic parameters defining the size and the structure of the members are limited to a practical range. However, the use of such member is not restricted to straight members or members within the specified range of parameters. In some structures, it may be necessary to use such members in a curved shape. Therefore, as a further study, the stability of curved members under axial compression as well as transverse loading must be studied. The behavior of members having parametric values outside the range specified in this study must be investigated.

In addition, the local and torsional buckling of such members must also be studied in detail.

REFERENCES

[1] Duleau A., “Essai théorique et expérimental sur la résistance du fer forgé, contenant des expériences ... avec des applications des résultats de ces expériences à l'art des constructions”, *V. Courcier*, 1820.

[2] Fairbairn W., “An Account of the Construction of the Britannia and Conway Tubular Bridges”, *John Weale et al.*, London, 1849.

[3] Zenkert D., “Sandwich Construction”, *EMAS Publishing*, Warley, England, 1997.

[4] Plantema F.J., “Sandwich Construction”, *John Wiley & Sons*, New York, 1966.

[5] Ettouney and Schmidt, “Finite Element Solutions of Deep Beams”, *Journal of Structural Engineering*, 109(7), July, 1983, p. 1569-1584.

[6] Mucichescu D.T., “Bounds for stiffness of prismatic beams”, *Journal of Structural Engineering*, 110(6), October, 1983, p. 1410-1414.

[7] Onu G., “Shear effect in Beam Stiffness Matrix”, *Journal of Structural Engineering*, 109(9), September, 1983, p. 2216-2221.

[8] Tessler A., and Dong S. B., “On a hierarchy of conforming Timoshenko beam elements”, *Computers and Structures*, 14, 1981, p. 335-344.

[9] Timoshenko S. P., "On the transverse vibrations of bars of uniform cross-section.", *Phil. Mag.*, 43, 1922, p. 125-131.

[10] Tessler A., and Hughes T. J. R., ”A three-node Mindlin plate element with improved transverse shear”, *Computer methods in applied mechanics and engineering*, 50 ,1985, p. 71-101.

[11] Tessler A., and Hughes, T. J. R. “An improved treatment of transverse shear in the Mindlin-type four-node quadrilateral element.”, *Computer methods in applied mechanics and engineering*, 39, 1983, p. 311-335.

[12] Oral S., “Anisoparametric Interpolation in Hybrid-Stress Timoshenko Beam Element”, *Journal of Structural Engineering*, 117(4), 1991, p. 1070-1078.

[13] Friedman Z., and Kosmatka J. B., “An improved two-node Timoshenko beam finite element.”, *Computers and Structures*, 47(3), 1993, p. 473–481.

[14] Kosmatka J. B., “An improved two-node finite element for stability and natural frequency of axial-loaded Timoshenko beams.”, *Computers and Structures*, 57(1), 1995, p. 141–149.

[15] Aydogan M., “Stiffness-matrix formulation of beams with shear effect on elastic foundation.”, *Journal of Structural Engineering*, 121(9), 1995, p. 1265–1270.

[16] Wang C. M., “Timoshenko beam-bending solutions in terms of Euler-Bernoulli solution.”, *Journal of Structural Engineering*, 121(6), 1995, p.763–765.

[17] Ortuzar J. M. and Samartin A. “Some consistent finite element formulations of 1-D beam models: A comparative study.”, *Advances in Engineering Software*, 29(7–9), 1998, p.667–678.

[18] Bazoune A. and Khulief Y. A. “Shape functions of three dimensional Timoshenko beam element.”, *Journal of Sound and Vibration*, 259(2), 2003, p. 473– 480.

[19] Frostig Y., Baruch M., Vilnay O., and Sheinman I. “High-order theory for sandwich-beam behavior with transversely flexible core.”, *Journal of Engineering Mechanics*., 118(5), 1992, p. 1026–1043.

[20] Frostig Y., and Baruch M. “High-order buckling analysis of sandwich beams with transversely flexible core.”, *Journal of Engineering Mechanics*., 119(3), 1993, p. 476–495.

[21] Sokolinsky V., and Frostig Y. “Boundary condition effects in buckling of ‘soft’ core sandwich panels.”, *Journal of Engineering Mechanics*, 125(8), 1999, p. 865– 874.

[22] Lee K. H., Xavier P. B., and Chew C. H. “Static response of unsymmetric sandwich beams using an improved zigzag model.”, *Composites Eng.*, 3(3), 1993, p. 235–248.

[23] Reddy J. N., “Mechanics of laminated composite plates”, *CRC*, Boca Raton, Fla, 2004.

[24] Perel V. Y., and Palazotto A. N., “Finite element formulation for cylindrical bending of a transversely compressible sandwich plate, based on assumed transverse strains.”, *Int. J. Solids Struct*., 38(30– 31), 2001, p. 5373–5409.

[25] Bathe K. J., ”Finite Element Procedures”, *Prentice Hall Inc.*, 2-3, 1996.

[26] “CSI Analysis Reference Manual For SAP2000, ETABS, and SAFE”, *Computers and Structures Inc.*, Oct. 2005.

[27] Computers & Engineering Company, “http://www.comp-engineering.com/ products/SAP2000/sap2000.html”, Last accessed date: 14.01.2009.

[28] Eurocode 3: “Design of Steel Structures”: ENV 1993-1-1: Part 1.1: General rules for buildings, CEN, 1992.